ELECTRON PARAMAGNETIC RESONANCE STUDY OF COPPER HALIDE TETRAZOLE COMPLEXES AND THE FREE RADICALS IN IRRADIATED STRONTIUM ACETATE HEMIHYDRATE

by

Robert Gary Gisch

United States
Naval Postgraduate School

THESIS

ELECTRON PARAMAGNETIC RESONANCE STUDY
OF COPPER HALIDE TETRAZOLE COMPLEXES AND THE
FREE RADICALS IN IRRADIATED STRONTIUM ACETATE
HEMIHYDRATE

by

Robert Gary Gisch

June 1969

Electron Paramagnetic Resonance Study of Copper Halide Tetrazole Complexes and the Free Radicals in Irradiated Strontium Acetate Hemihydrate

by

Robert Gary Gisch
Lieutenant (junior grade), United States Navy
B.S., Marquette University, 1968

Submitted in partial fulfillment of the
requirements for the degree of

MASTER OF SCIENCE IN CHEMISTRY

from the

NAVAL POSTGRADUATE SCHOOL
June 1969

ABSTRACT

An EPR study of copper halide tetrazole complexes and x-irradiated strontium acetate hemihydrate has been made. The powder spectra of some of the tetrazole complexes exhibited temperature dependent narrowing and broadening. The one-electron population of the copper d orbital involved in bonding to 2-methyl-5-amino tetrazole has been found to be 0.56 and 0.47, respectively for the chloride and bromide complexes. The g value for these two complexes are consistent with the proposed planar polymeric structure for 2-substituted tetrazole-copper complexes. The species present in single crystals of strontium acetate hemihydrate irradiated and observed at liquid nitrogen temperature to -100^{o} C has a spectrum of four lines of 1:3:3:1 intensity ratio and $a^{CH_3} = 11.0$ gauss. Temperature dependent exchange behavior of the spectrum for this species is observed and attributed to a rotating methyl group which was found to have $\Delta H^{\neq} = 3.0 \pm 0.3 \frac{kcal}{mole}$ and $\Delta S^{\neq} = 6.0 \pm 0.3$ cal/mole deg for internal rotation. The species present at room temperature has an eight line spectrum consisting of two 1:3:3:1 intensity ratio patterns with $a^{CH_3} = 25.2$ and $a^{H} = 21.3$ gauss. Molecular orbital calculations using the CNDO approximation were performed and possible fragments responsible for these spectra are suggested.

TABLE OF CONTENTS

LIST OF TABLES

LIST OF ILLUSTRATIONS

ACKNOWLEDGEMENT

The author wishes to thank Professor William Tolles for his help and encouragement in bringing this research to a successful conclusion.

I. INTRODUCTION

The work reported in this thesis consists of two parts. The first part, Sections II through VI inclusive, contains the results of research on copper halide-tetrazole complexes. The second part, which encompasses the rest of the thesis, examines the problem of the paramagnetic fragments produced in strontium acetate hemihydrate by x-irradiation.

The tetrazole work was suggested by Dr. H. B. Jonassen of the Chemistry Department of Tulane University, New Orleans, Louisiana, to provide information to supplement that already gathered by other means to study the structure of the copper halide tetrazole complexes and the coordination of the tetrazoles to the copper (II) in the complex. The radiation damage work on strontium acetate was begun at the conclusion of the copper tetrazole work with the purpose of obtaining information about the mechanism of radiation damage in crystals. This work has resulted in the discovery of free radical fragments not previously reported for a crystal of this type [25].

For each section, the thesis is written so that the reader is given the theory and background necessary to understand and appreciate the reported results in the context of current research in the areas of transition metal-tetrazole complexes and radiation damage studies of organic crystals.

II. ESR OF TRANSITION METALS

Electron spin resonance (ESR) measures the absorption spectra which arise from transitions between energy states. The energy states are the result of an interaction of the unperturbed energy states of the paramagnetic species with a magnetic field. In this section the theory of these states and their description by a spin Hamiltonian will be discussed. The theory of the g tensor for transition metals as developed by Carrington and McLachlan [1] will also be considered.

Elementary quantum mechanics provides the following relationship for calculating the average value of a property of a quantum mechanical system:

$$\langle Q \rangle = \int \psi^* \theta \psi \, d\tau$$

where θ is an operator for the property Q whose average value is to be calculated and ψ is the spatial wave function for the system. ESR is used to determine the energy levels of a system. An extension of the above relationship to a system with several energy levels can be made without too much difficulty. The operator for the energy is called the spin Hamiltonian which is, for one electron:

$$\mathcal{H}_s = \beta \vec{H} \cdot \vec{\vec{g}} \cdot \vec{s} - \sum_i \gamma_i \hbar \vec{H} \cdot \vec{I}_i + \sum_i \vec{S} \cdot \vec{\vec{A}}_i \cdot \vec{I}_i$$

In essence, the terms in the Hamiltonian describe the contribution to the total energy which are made by interactions of the electrons and nuclei with the external magnetic field and with one another. The first term is the electron Zeeman term. It represents the Zeeman energy, the energy of interaction of the electron spin moment with the external

magnetic field. β is the Bohr magneton, S is the electron spin and g is the spectroscopic splitting tensor which may well be anisotropic. The second term is a summation of the Zeeman energies of the nuclei. I_i is the spin of the ith nucleus and γ_i is the gyromagnetic ratio of the ith nucleus. The third term represents the summation of the energy of the hyperfine interaction between the electron spin and the spin of the ith nucleus. $\vec{\vec{A}}_i$ is the hyperfine interaction tensor. In this section only the first term in the Hamiltonian will be considered:

$$\mathcal{H}_s = \beta\vec{H} \cdot \vec{\vec{g}} \cdot \vec{S} = (H_x H_y H_z) \begin{pmatrix} g_{xx} & g_{xy} & g_{xz} \\ g_{yx} & g_{yy} & g_{yz} \\ g_{zx} & g_{zy} & g_{zz} \end{pmatrix} \begin{pmatrix} S_x \\ S_y \\ S_z \end{pmatrix}$$

In the absence of spin-orbit coupling the g tensor is isotropic and S represents the true spin of a free electron. However, consider the case where g is anisotropic, since this is the case which is almost always encountered with transition metal complexes. It naturally follows from above that an anisotropic g tensor implies that S cannot possibly represent the true spin. Instead, for anisotropic g,

$$\mathcal{H}_s = \beta\vec{H} \cdot \vec{\vec{g}} \cdot \vec{\hat{S}}$$

where $\vec{\hat{S}}$ is called the fictitious spin.

The reader might recall the fact that in the presence of a magnetic field, there is an interaction between H and L, the orbital angular momentum of the electron. In this case, the true form of the Hamiltonian for the interaction of an unpaired electron with a magnetic field is

$$\mathcal{H}_s = \beta\vec{H} \cdot \vec{L} + g_e\beta\vec{H} \cdot \vec{S}$$

where g_e is the free electron g = 2.0023. The two forms of H_s are

equivalent. This fact is used to develop some mathematical relationships which will help in the understanding of the anisotropy of the g tensor.

It can be shown that the only way an odd electron can acquire orbital angular momentum is through the effect of spin-orbit coupling, which is represented by

$$\zeta \vec{L} \cdot \vec{S}$$

where ζ is called the spin-orbit coupling constant, the value of which may be extracted from atomic spectra.

First order perturbation theory allows the calculation of modified ground state wave functions $< + 1$ and $< - 1$. $\zeta \vec{L} \cdot \vec{S}$ is the perturbation operator which mixes the ground state wave functions $\langle \psi_o, \alpha |$ and $\langle \psi_o, \beta |$ with excited states. $|\alpha\rangle$ and $|\beta\rangle$ are the spin functions (for notation, and details of development, see [1]).

The fictitious spin can now be defined as follows:

$$\hat{S}_z | + \rangle = \tfrac{1}{2} | + \rangle \qquad \hat{S}_x | + \rangle = \tfrac{1}{2} | - \rangle$$

$$\hat{S}_z | - \rangle = -\tfrac{1}{2} | - \rangle \qquad \hat{S}_y | + \rangle = \tfrac{1}{2} i | - \rangle$$

In a magnetic field along the i axis (i = x,y,z)

$$\mathcal{H}_s = \alpha H_i \cdot (g_{ix} \hat{S}_x + g_{iy} \hat{S}_y + g_{iz} \hat{S}_z) .$$

Setting up the matrix representation of this form of $\mathcal{H}_s$ in the basis $| + \rangle$, $| - \rangle$ and comparing it with the matrix representation of $\mathcal{H}_s = \beta H \cdot L + g_e \beta H \cdot S$ in the same basis, it is found that:

$$g_{xx} = g_e - 2 \sum_n \frac{\langle 0|L_x|n\rangle\langle n|L_x|0\rangle}{\Delta E_n}$$

$$g_{yy} = g_e - 2 \sum_n \frac{\langle 0|L_y|n\rangle\langle n|L_y|0\rangle}{\Delta E_n}$$

$$g_{zz} = g_e - 2 \sum_n \frac{\langle 0|L_z|n\rangle\langle n|L_z|0\rangle}{\Delta E_n}$$

where ΔE_n is the difference in energies between the ground state electronic level and the nth electronic level. The value of ΔE_n may be extracted from optical spectra.

III. EXPERIMENTAL SPECTRA AND THEIR ANALYSIS

A. SINGLE CRYSTAL METHOD

Of the methods available for studying paramagnetic species in solids, the single crystal method provides the best results. The species to be studied is regularly oriented relative to the crystal axes, and this provides the opportunity to rotate the crystal in the magnetic field and measure the anisotropic interactions, giving valuable information about structure of the paramagnetic species.

The type of spectrum obtained is dependent upon the orientation of the external magnetic field with respect to the paramagnetic species, and the number and type of different species in the crystal. In addition, there may be more than one magnetically distinct site for a particular species in the lattice. Fortunately, there is usually a particular orientation for the magnetic field which results in a spectrum which is relatively easy to interpret and allows the experimentalist to extract the desired information. This information enables the experimentalist to find the orientation of the principal axis system of the species with respect to the crystal axis system. It is in the principal axis system that the A and g tensors are diagonal. Since each tensor has three diagonal components, there are three orthogonal directions for the magnetic field along which the values of g_{xx}, g_{yy}, and g_{zz} may be extracted. A_{xx}, A_{yy}, and A_{zz} may sometimes also be extracted.

B. THE POWDER AND FROZEN SOLUTION METHODS

When single crystals of the material to be studied cannot be grown, or when the information cannot be extracted from single crystal studies, then the powder or the frozen solution "glass" method is utilized. In both the powder and glass, the paramagnetic species are randomly oriented with respect to the magnetic field and absorb over a wide range of magnetic field. The glass provides a method for diluting the species in order to reduce the line broadening effects which are caused by the interaction of neighboring complexes.

C. LINE WIDTHS

There are three factors which McGarvey [2] considers that can contribute to the width of ESR absorption lines. They are:

(a) Anisotropy of g factors and hyperfine interactions or spin-interactions.

(b) Interaction with magnetic dipoles of neighboring electronic and nuclear spins.

(c) Spin-lattice relaxation times.

The first factor is important for powder samples in which the small crystals are randomly oriented. In this case, the method needed to obtain narrower lines is to grow single crystals. If this cannot be done, then it is sometimes possible to extract the information from the shape of the broad powder spectrum.

The second factor can often be a significant one, since magnetic fields produced by dipoles over distances of a few angstroms are very large. These large internal magnetic fields coupled with the external magnetic field may cause the local field at the site of the paramagnetic

species to vary greatly. Since the field of a magnetic dipole is inversely proportional to the third power of the distance, the best way to reduce this broadening effect is to place the species in an isomorphic diamagnetic crystal or to use the glass method.

The length of time associated with the relaxation of an excited spin state to a thermal equilibrium spin state given by Boltzmann statistics is called the spin-lattice relaxation time. The relaxation is accomplished by a transfer of energy between the magnetic spins and the vibrational energy of the crystal lattice to which the spins are coupled. For systems where the spins are strongly coupled to the vibrational modes, the lifetime of a given magnetic state is short, resulting in an uncertainty in the energy which manifests itself as a broad absorption line. This broadening mechanism is strongly dependent on the temperature, so that the lines broadened in this manner can be sharpened by lowering the temperature of the sample. Extremely short relaxation times often occur when the paramagnetic species has an electronic excited state just above the ground state. In cases of this sort, it is often necessary to go to liquid helium temperature.

IV. BACKGROUND ON TRANSITION METAL-TETRAZOLE COMPLEXES

Tetrazoles are five-membered, heterocyclic ring compounds which contain one carbon and four nitrogen atoms linked by three single and two double bonds. The parent compound may exist in tautomeric forms I and II. It was reported by Lounsburg [3] that 97% of tetrazole is of the form I:

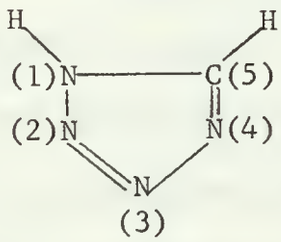

I

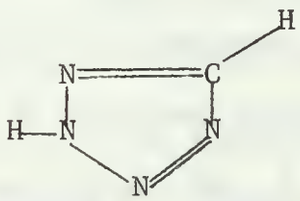

II

The tetrazole ring is unusual in that the only two points of substitution are in positions 1 or 2 and 5. Chemical investigations have shown that the tetrazoles are nucleophilic reagents and that the nucleophilic character varies with the nature and position of the groups substituted on the ring.

Jarvis [4] investigated the crystal structure of a 1:1 complex of copper (II) chloride and 1,2,4 triazole. He reported the unit cell dimension to be

$$a = 6.81, \quad b = 11.39, \quad c = 7.13 \text{ Å} ; \quad \beta = 96^{\circ} 58'$$

The space group is I2/c and contains four units of $C_2N_3H_3 \cdot CuCl_2$. The copper atom has a distorted octahedral coordination group consisting of two N at 1.98 Å, two Cl at 2.34 Å, and two Cl at 2.77 Å. The structural unit is an infinite chain in which octahedral groups, joined by sharing edges, are also linked by triazole molecules.

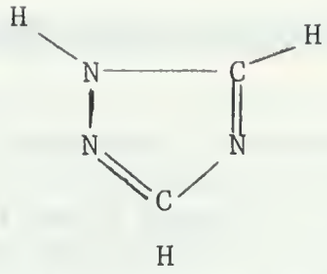

1,2,4 TRIAZOLE

Jonassen [5] reported the preparation of a number of copper halide tetrazole complexes of differing compositions. He determined that the copper halide complexes of 1-substituted tetrazoles have the composition Cu X_2T_2 and postulated a structure analagous to the triazole structural unit for them. The copper halide complexes of 2-substituted tetrazoles have the composition CuX_2T. The proposed structures of the 1 and 2-substituted tetrazole complexes of copper (II) halides, respectively, are shown in the top and bottom of Fig. 1. Jonassen also carried out a reduction reaction on several of the copper tetrazole complexes with acetone and discovered that the product of the reaction was always a CuXT, regardless of the composition of the starting material. He reasoned that in CuXT, polymeric CuCl chains are present with bridging tetrazole groups forming four coordinated copper (I) species.

Garber and Brubaker [6], reporting the results of their work on bis(1-methyl-5-tetrazoyl) and bis(1-cyclohexyl-5-tetrazoyl) nickel (II), stated that the reflectance spectra of these complexes indicated that the nickel is in an octahedral environment. They also concluded that the insolubility of these complexes in all common solvents suggest a polymeric structure.

Brubaker [7] carried out continuous variation experiments on 5-aminotetrazolato-copper (II) and showed that there is a 1:2 interaction of copper (II) with the tetrazole according to the mechanism:

$$HT = H^{+} + T^{-} \qquad K_a = 6.8 \times 10^{-7}$$

$$Cu^{2+} + 2T^{-} = CuT_2$$

He determined the formation constant of the association reaction to be $K_f = 1.3 \times 10^{12}$. Infrared analysis of this complex indicated that coordination of the tetrazole to the copper (II) does not involve the amino group. Jonassen [5], reporting on this same complex, stated that the tetrazole nitrogens form dative bonds with the copper (II) above and below the plane, thus forming a bridged structure.

Bowers and Popov [8] worked on pentamethylene tetrazole complexes of copper halide and compared the results with work carried out previously on $Cu(PMT)_6(ClO_4)_2$. They found that PMT is not a strong donor ligand and that at most, two PMT coordinate with Cu(II) in the halide complex as compared with six PMT with the perchlorate complex. In a few cases, they discovered solubilization of complexes when the solvent had strong donor properties. They found an abnormally low magnetic moment for the complex which is indicative of copper-copper bonding, but they concluded that their data did not allow an unambiguous identification of such bonds. They also concluded, from magnetic and spectral evidence, that the copper (II) in $Cu(PMT)X_2$ is in an octahedral environment.

Kuska, D'Itri and Popov [9] investigated the powder spectrum of $Cu(PMT)_6(ClO_4)_2$ and from the observable nitrogen superhyperfine splitting and comparison with optical and ESR data for other copper complexes,

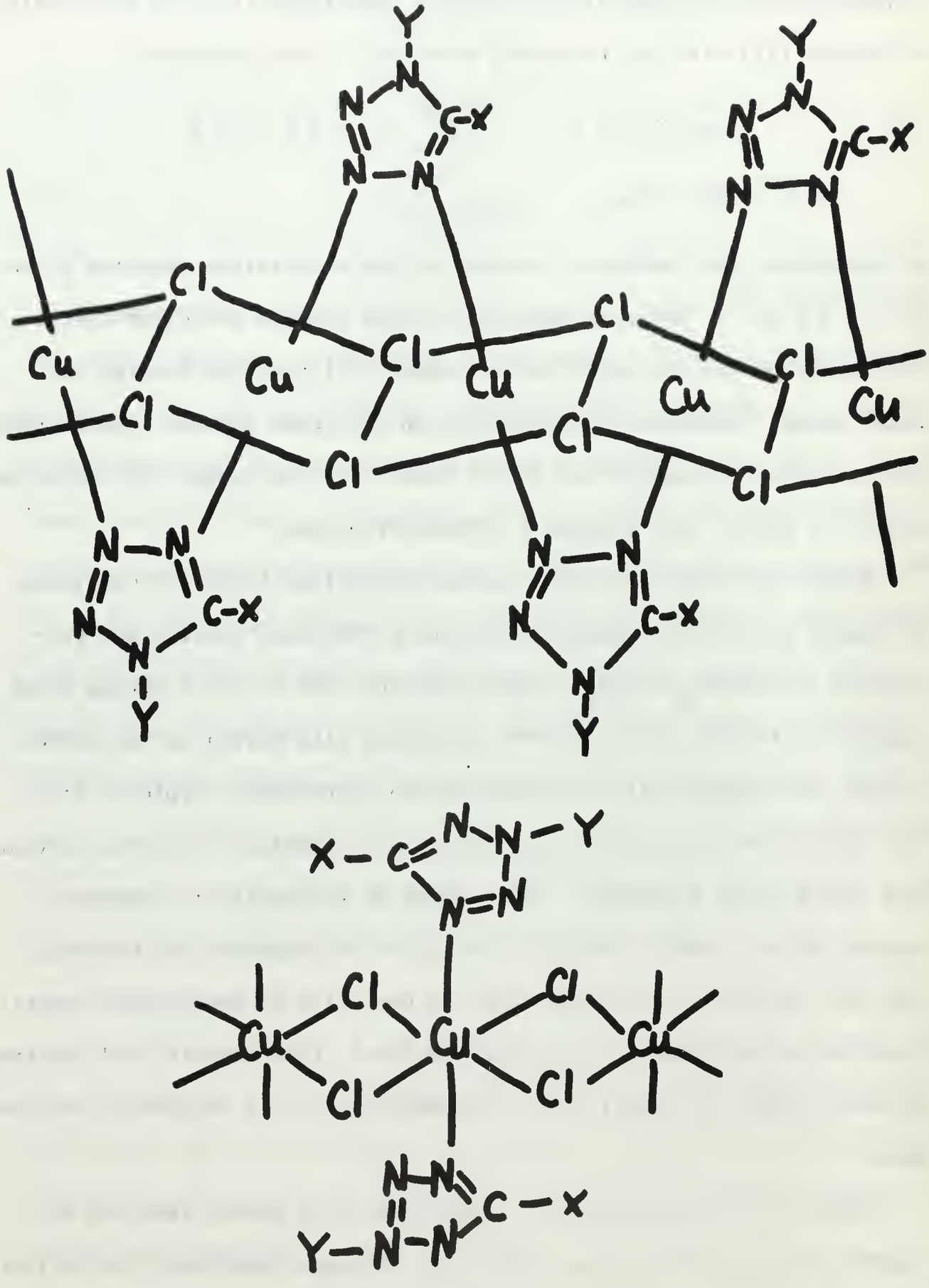

FIGURE 1. Proposed structures of 1-substituted tetrazoles (top) and 2-substituted tetrazoles (bottom) after Jonassen [5].

concluded that the bonding of the PMT ligand is 80% ionic. They also concluded that the PMT nitrogen-copper (II) orbitals have a greater percentage of s character than the assigned sp^2 hybridization.

V. MATERIALS AND EQUIPMENT

A. OBTAINING THE DATA

The copper tetrazole complexes studied were supplied by Dr. R. A. Henry of the Chemistry Division, Naval Weapons Center, China Lake, California. Their purity was checked by Galbraith Laboratories, Inc., Knoxville, Tennessee. The analytical data indicated that the samples were of sufficiently high purity for this study [5].

The ESR spectra were obtained with a Varian V-4502-06 X-band ESR spectrometer utilizing 100 kc/sec modulation with a nine inch magnet and field-dial regulation. The cavity was a conventional reflection type cavity, equipped with a Varian variable temperature control unit which allowed temperature regulation down to 90^{o} K. For liquid helium work, the same type of spectometer modified to accomodate a liquid helium dewar and pumping system was used. This system allowed observation of the sample at 3^{o} K.

The powder spectra were obtained by placing the powder in 4 mm O.D., 3 mm I.D. quartz tubing sealed at one end. The frozen solution spectra work was accomplished in a similar manner by filling the sealed quartz tubing with a solution of the tetrazole complex and then freezing it with the temperature control unit. The single crystal work was accomplished by rotating the sample on the gear wheel of a goniometer, an instrument which gives the experimenter the freedom to orient the crystal about two axes, the axes vertical to and horizontal with the pole faces of the magnet.

The data was taken from the EPR spectra for the powder and frozen solution method by using the baseline of the spectrum as a reference and measuring the linewidths and coupling constants with a ruler graduated in hundredths of an inch. The data for the single crystal work was taken from the oscilloscope display of the absorption spectrum. The orientation of the single crystal was changed with the goniometer while observing the scope display, and data taken when the absorption line reached an extreme or inflection point of the magnetic field at which resonance was occurring. The resonance fields were read off the field dial by centering the absorption line on the crosshairs of the oscilloscope display.

The calibration of the field dial with the linear scale of the recorder was accomplished by inserting a solid mixture of 0.1% $MnCl_2$ in MgO into the cavity and comparing the field dial readings and linear measurements of the coupling constant from the recorder with the coupling constant as determined with an NMR probe.

For the single crystal work, each piece of data consisted of two angles of rotation, a resonance field, and a linewidth. The data was cataloged with a stereographic net, and the three orientations at which data was taken for each single crystal were confirmed to be orthogonal to one another on the stereographic net.

B. CATALOGING THE DATA

Suppose a paramagnetic single crystal is to be studied. This crystal has a definite form which allows for definition of a three dimensional orthogonal crystal axis system relative to the crystal faces. The experimentalist has the job of finding the orientation of the principal

axis system with respect to the crystal axis system. Consider this process from a different viewpoint. Reorienting the crystal in a fixed magnetic field is equivalent to reorienting the magnetic field with respect to a fixed crystal axis system.

Consider the crystal axis system X Y Z in Fig. 2. It is easy to see that all points in space may be convered by rotating a given vector through all angles of θ and ϕ. Suppose the experimenter wants to collect data from the paramagnetic crystal over several magnetic field orientations. The stereographic net provides a convenient method of cataloging the information obtained. Each value of θ and ϕ corresponds to one point on the stereographic net. Figure 2 gives the three dimensional picture of a principal axis system X' Y' Z' relative to the crystal axis system X Y Z . The representation of the same points on the stereographic net appears directly above for comparison. The stereographic net covers all points over a hemisphere. Because the ESR spectrum remains unchanged by a reversal of the magnetic field direction, corresponding points on the two hemispheres are equivalent.

The procedure for finding X' Y' Z' consists of taking data over several orientations of the magnetic field and cataloging the data with the stereographic net. Once this is done, a reasonable guess is made at the three orthogonal points on the net which, in consideration of the data distribution on the net, seem most likely to represent X', Y', and Z'. The initial guesses are then fed into a computer program for further refinement.

The stereographic net thus provides a convenient method for cataloging data and providing the experimenter with an overall picture of the data distribution which leads to an initial guess at the orientation of the principal axis system relative to the crystal axis system.

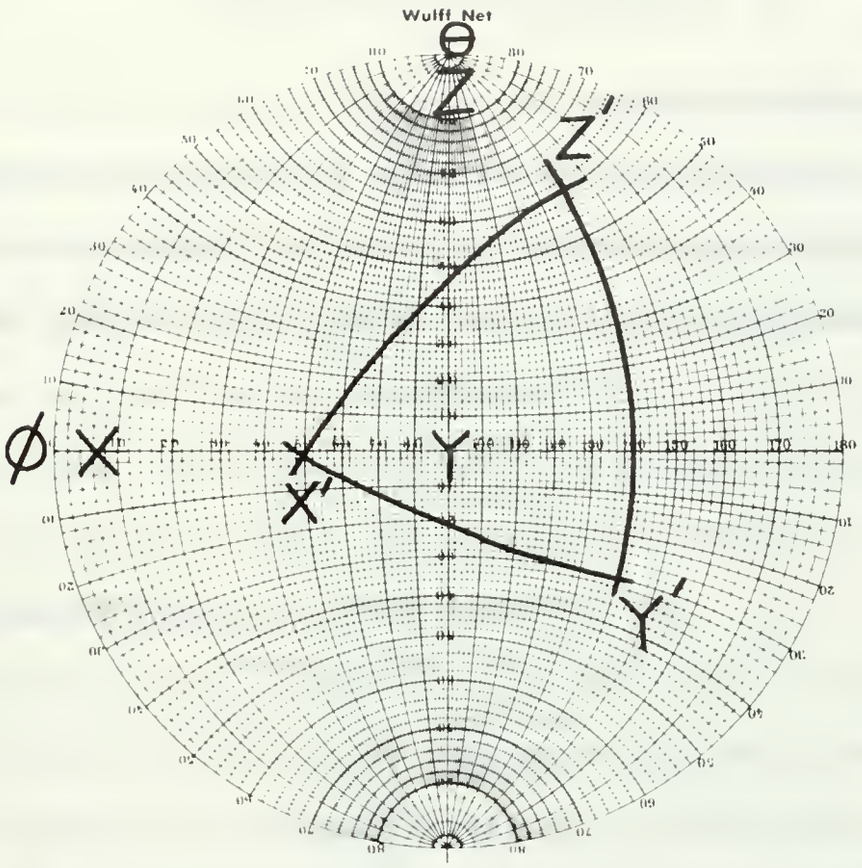

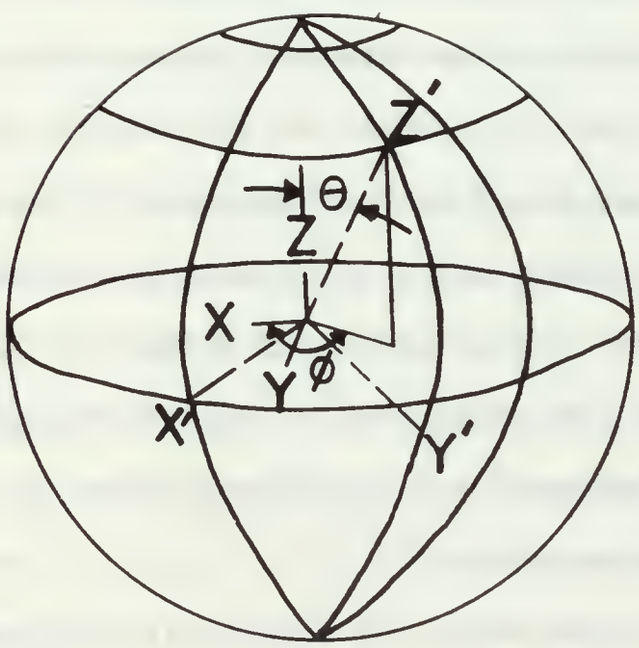

FIGURE 2

VI. EXPERIMENTAL WORK AND RESULTS

A. FROZEN SOLUTION SPECTRA

Frozen solution work was undertaken in order to study those complexes which did not grow single crystals or for which the powder spectra were unsatisfactory. The following organic solvents were tried:

Isopentane
Glycerine
Benzene
Chloroform
Diethyl ether and mixtures of these
Methyl ethyl ketone
Acetone
Ethanol
Dimethylformamide

A small amount of the powder was placed in a beaker and the solvent added at room temperature. Upon very careful attempts to dissolve the complexes in the solvents, it was discovered that in almost all attempts either the complex did not dissolve at all or what at first appearances seemed to be dissolution of the complex in the solvent was in actuality only a fine dispersion of the powder in the solvent. A few of the complexes did dissolve to a very slight degree, however, the spectra which were obtained in the glass at 113^{o} K were impossible to interpret due to the small signal to noise ratio and other complicating effects.

The only solvent which did dissolve all of the copper halide tetrazole complexes was dimethylformamide. The copper bromide tetrazoles gave quite simple spectra in DMF whereas the spectra of the copper chloride tetrazoles showed several overlapping peaks which was indicative

of more than one distinct position in the frozen lattice of dimenthylformamide.

Three typical spectra of frozen DMF solutions of copper bromide tetrazoles are shown in Fig. 3. The top spectrum is that of copper bromide dissolved in DMF. It was used as a reference with which to compare the other spectra. The other two spectra exemplify, respectively, the phenomena of broadening of the spectral lines and shifting of the spectral lines. The middle spectrum is 1-benzyl-5-amino tetrazole with copper (II) bromide in DMF, and the bottom spectrum is 1,5 tetramethylene tetrazole with copper (II) bromide in DMF.

The fact that the complexes did not dissolve to an appreciable extent in all but DMF substantiates the conclusion of previous workers that the complexes have a polymeric structure which does not break down easily. The dissolution in DMF seems to imply that DMF coordinates more strongly to copper than do the tetrazoles. The data in Table 1 leads to a partial confirmation of this fact, and also allows for some other conclusions.

Previous workers [9] concluded that the bonding of the PMT ligand to copper is 80% ionic and that PMT is a poor donor. Data in Table 1 indicates that the PMT ligand has been replaced by DMF and that the same thing has happened for some of the other complexes. This is not, however, the case for all the complexes as can be seen. For the two complexes which exhibit values of ΔH and A different from those listed for the copper bromide case, it must be concluded that the tetrazole ligands have not been completely replaced by the DMF, but rather, a type of coordination still exists between the copper and the tetrazoles. The difference in ΔH values is due to the difference in the ligand

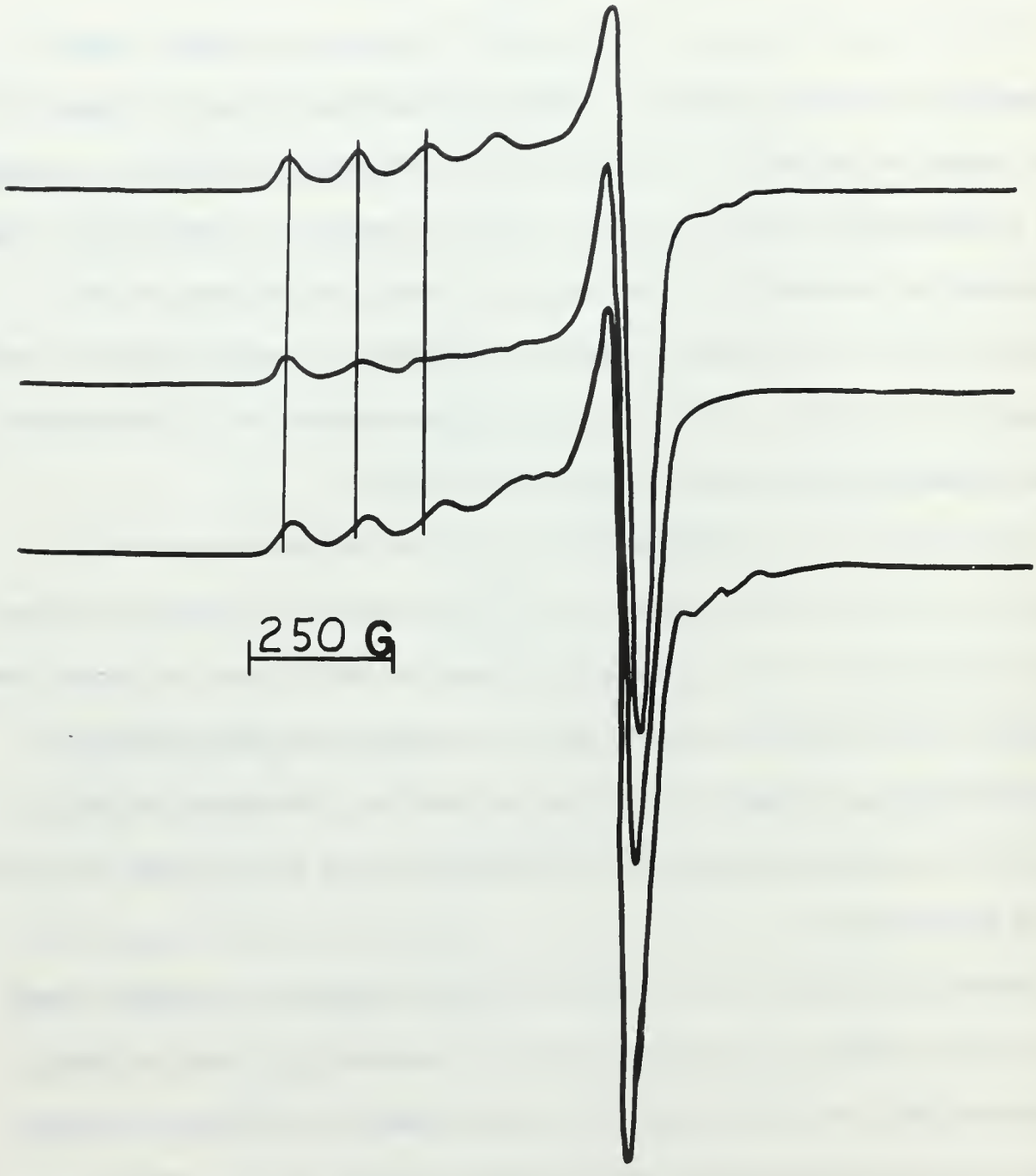

FIGURE 3

COMPLEX	ΔH (gauss)	AVERAGE A (gauss)*
$CuBr_2$	448 ± 6	119 ± 6^3
2 phenyl	442 ± 6	119 ± 6^3
1 Methyl-5-ethyl	448 ± 6	116 ± 6^3
1,5 pentamethylene	448 ± 8	119 ± 8^2
2 methyl-5-amino	lines too broad to be observed	
1 benzyl-5-amino	lines too broad to be observed	
1 methyl-5-amino	lines too broad to be observed	
1,5 tetramethylene	416 ± 8	139 ± 8^2
1,5 trimethylene	412 ± 8	138 ± 8^2

*Superscript indicates the number of A values which were averaged.

In cases where less than three values were averaged, the remaining A values were lost to line broadening effects.

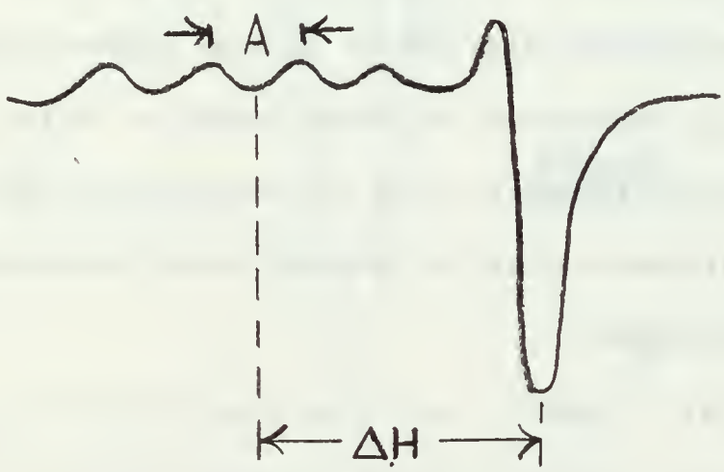

TABLE 1. $CuBr_2$-Tetrazole Complexes in Frozen Solution of Dimethylformamide

splitting of the electronic levels of the copper ion. Since the ΔH values are inversely proportional to the ligand splitting, ΔE (see Introduction), larger ΔH values imply a smaller splitting by the ligand. The A values are a measure of the localization of the electron in the copper orbital. The larger the A value, the more the electron is localized.

B. POWDER SPECTRA

Due to the lack of success in the attempts to grow single crystals of the complexes supplied, spectra were taken of the complexes in their powder or microcrystalline form. The resulting spectra all exhibited extremely broad lines at room temperature. Initially attributing the broad lines simply to spin-lattice relaxation effects, a series of experiments was performed on four particular complexes which exhibited anisotropic line shapes at room temperature. These experiments revealed temperature dependent behavior of the spectra of all four complexes. Figure 4 shows the variation of the powder spectra of the four different tetrazole complexes with temperature. The four complexes studied were:

Figure 4A: 1-methyl-5-ethyl tetrazole with $CuCl_2$

Figure 4B: 1-methyl-5-amino tetrazole with $CuCl_2$

Figure 4C: 1,5-pentamethylene tetrazole with $CuBr_2$

Figure 4D: 1-benzyl-5-amino tetrazole with $Cu\ Br_2$

Encouraged by the fact that for some of the complexes, the spectral lines narrowed at lower temperature, it was decided to try work at liquid helium temperature. Initial preparations with a spectrometer similar to that used for the liquid nitrogen work proceeded slowly and

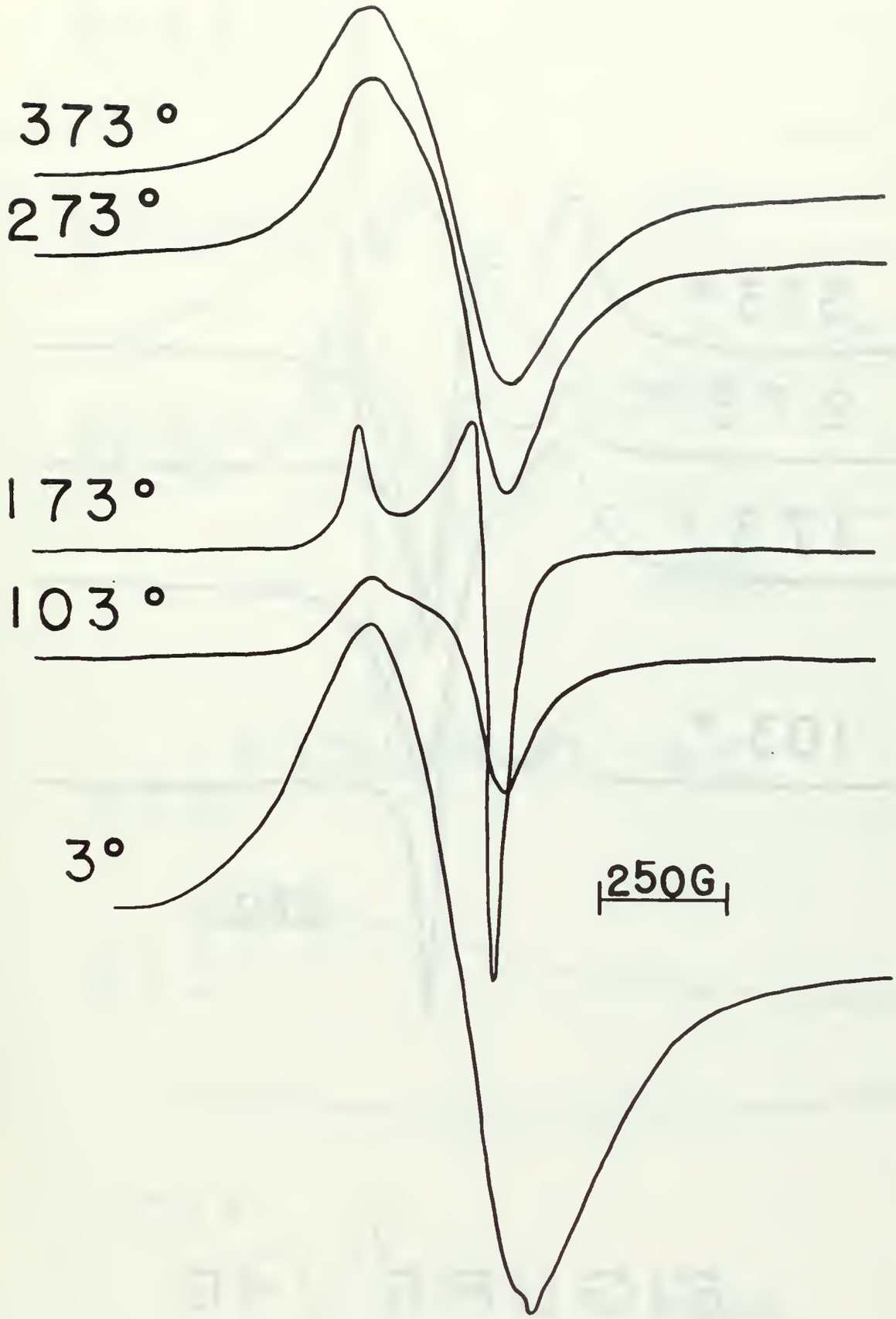

FIGURE 4A

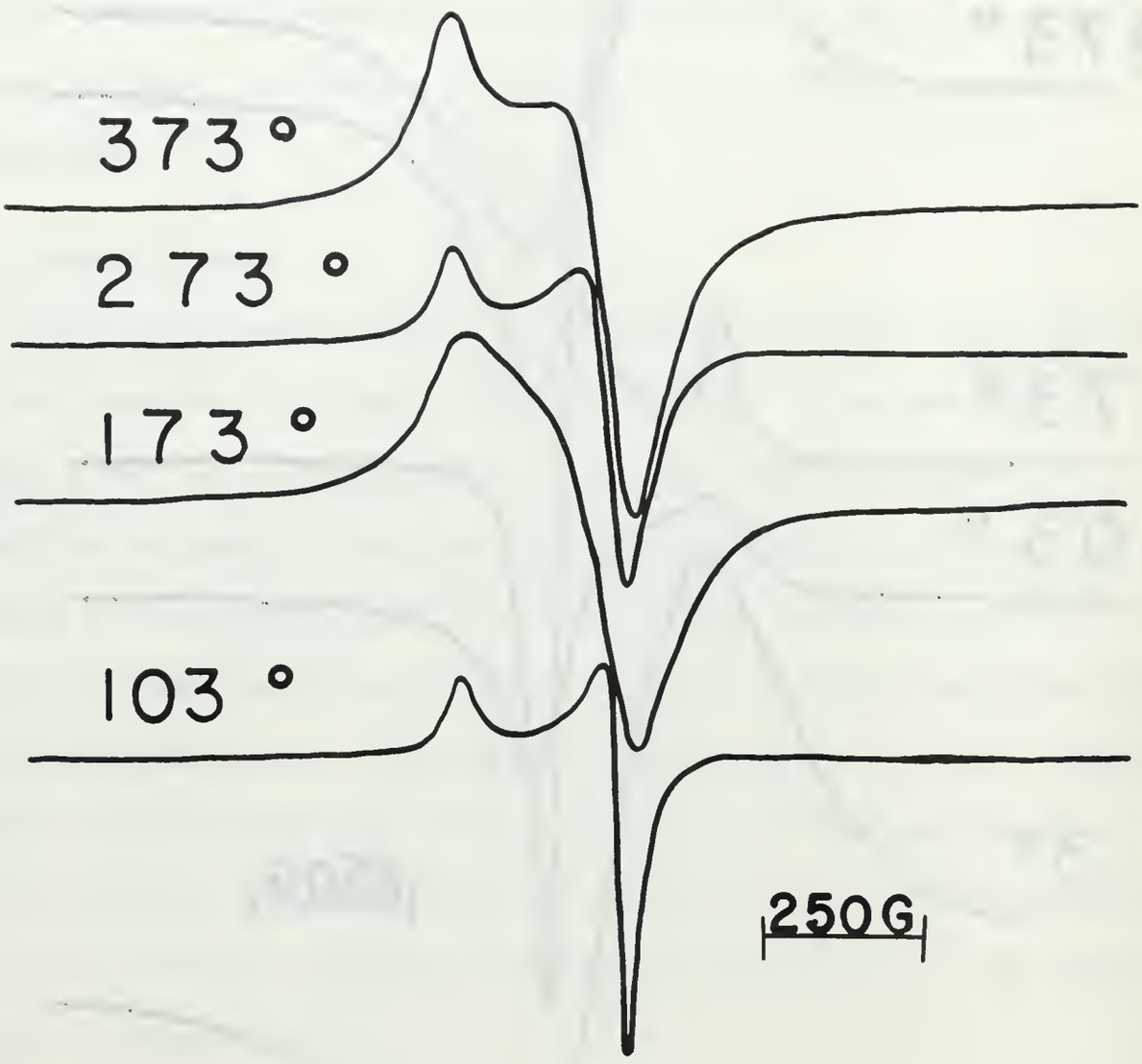

FIGURE 4B

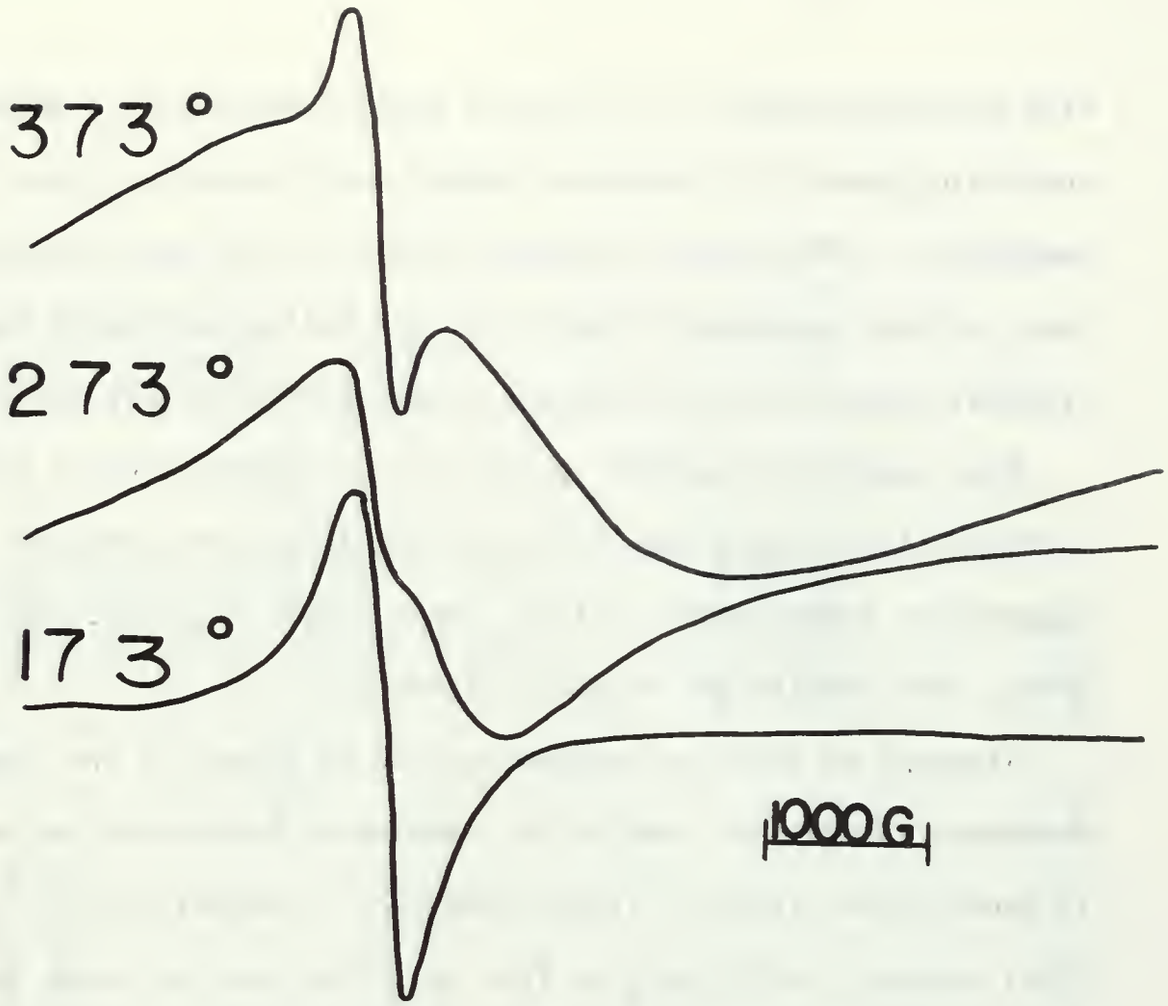

FIGURE 4C

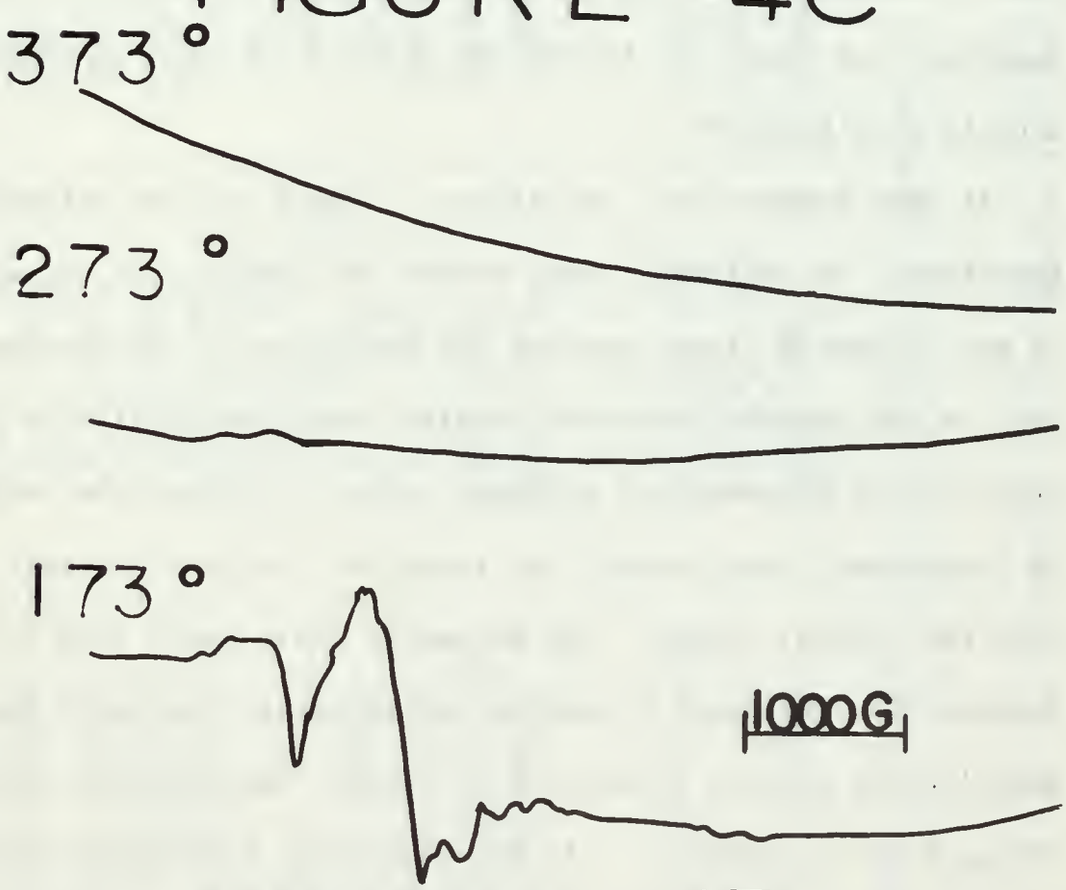

FIGURE 4D

with much difficulty, but finally a powder spectrum of 1-methyl-5-amino tetrazole copper (II) chloride complex was obtained at liquid helium temperature. The result is shown in Fig. 4A. It was concluded on the basis of this experiment that the liquid helium work would bear little fruitful results, and so efforts in this direction were terminated.

Room temperature powder spectra of the complexes which exhibited isotropic line shapes were taken and the line width measured. Room temperature powder spectra of the three copper (I) complexes were also taken. The results are listed in Table 2.

Although no positive explanation can be given for the temperature dependent behavior of some of the complexes, hypotheses may be advanced to explain the effects. Typical behavior is exemplified by 1-methyl-5-ethyl tetrazole with $CuCl_2$ in Fig. 4A. The spectrum seems to alternately broaden and narrow as the temperature is raised or lowered. The importance of some line broadening effects will now be considered to explain this behavior.

At high temperature, the effects of spin lattice relaxation are important. In addition, there exists the possibility of rapid exchange of the tetrazole ligand between two positions it could occupy (Fig. 1, top) in the puckered polymeric chain. This possibility is advanced in light of the discovery of previous workers [9] that the tetrazole ligand is in general a poor donor, and therefore does not interact strongly with the central copper. The polymeric chain would then be free to dynamically "repucker" by making and breaking bonds with the tetrazole. Spin-lattice effects would tend to broaden the spectral line and exchange tend to narrow it. At any particular temperature the dominance of one effect or the other would depend upon the structure of the

Position and kind of substituents on tetrazole	Composition of complex	Microscopic Appearance	Lineshape	Linewidth (gauss)
1-methyl-5-amino	$C_2H_5N_5$ $CuBr_2$	microcrystalline	isotropic	280 ± 9
1-benzyl-5-amino	$C_8H_9N_5$ $CuCl_2$	microcrystalline	isotropic	376 ± 9
1-methyl-5-ethyl	$C_4H_8N_4$ $CuBr_2$	powder	isotropic	252 ± 9
1,5-trimethylene	$C_4H_6N_4$ $CuBr_2$	powder	isotropic	497 ± 18
1,5-tetramethylene	$C_5H_8N_4$ $CuBr_2$	powder	isotropic	296 ± 18
2-phenyl	$2(C_7H_6N_4)$ $CuBr_2$	powder	anisotropic, shouldered	
2-phenyl	$2\ (C_7H_6N_4)$ $CuCl_2$	powder	anisotropic	
1-benzyl-5-amino	$C_4H_8N_4$ $CuBr_2$	microcrystalline	*	
1-methyl-5-ethyl	$C_4H_8N_4$ $CuCl_2$	powder	*	
1,5-pentamethylene	$C_6H_{10}N_4$ $CuBr_2$	powder	*	
1-methyl-5-amino	$C_2H_5N_5$ $CuCl_2$	powder	*	
2 - methyl-5-amino	$2(C_2H_5N_5)$ $CuBr$	powder	anisotropic	
2-phenyl	$2(C_7H_6N_4)$ $CuBr$	Powder	isotropic	462 ± 18
1-benzyl-5-amino	$C_8H_9N_5$ $CuBr$	powder	isotropic	323 ± 18

* Observed to show temperature dependent behavior

TABLE 2. Powder Spectra of Copper Halide Tetrazole Complexes

complex and the temperature dependence of the exchange mechanism. At lower temperatures, where the spin-lattice effects are greatly diminished and the lattice vibrations are very small, it is possible for the copper atoms to be close enough so that the electron is affected by both copper nuclei. This effect leads to dipolar relaxation and line broadening.

C. SINGLE CRYSTAL WORK

Of the many copper halide tetrazole complexes supplied by R. A. Henry of China Lake, only the 2-methyl-5-amino copper (II) chloride and bromide tetrazole complexes were in the form of crystalline chips large enough to be treated as single crystals. Numerous attempts at growing single crystals of the other complexes were made, and all but one attempt met with failure. The conventional method of growing crystals by slow evaporation from solution was impractical because the copper halide tetrazole complexes which were supplied were insoluble in all common organic solvents tried. Basically, all of the techniques for growing single crystals were based on the method of slow diffusion of the copper halide and the tetrazole dissolved in a suitable solvent. The slow diffusion technique was necessary because of the tendency of the complexes to immediately precipitate when a solution of tetrazole in solvent was poured into a solution of copper halide in the same solvent. The complexes have a very large formation constant [7].

The successful attempt at growing a single crystal of 2-methyl-5-amino copper chloride tetrazole complex yielded a crystal approximately ten times the size of any of the small crystals initially supplied from China Lake. A few grams of copper chloride was placed in the bottom of a long pyrex tube sealed at one end. The tube was filled with glass wool and a few grams of the 2-methyl-5-amino tetrazole placed on top of

the column of glass wool. The entire tube was filled with absolute ethanol and then stoppered and allowed to stand at room temperature. After a period of two months, a crystal about the size of a pea was observed to be clinging to the column of glass wool. Due to the time period involved in this technique, it was not tried with other tetrazoles. Of all the techniques for growing the single crystals of copper halide tetrazoles, this one showed the most promise. However, the complex from which the crystal was grown had already grown smaller single crystals. This was not the case for the rest of the complexes which came in powder or microcrystalline form.

The results of the single crystal work with the two complexes mentioned above is reported in Table 3. The spectra of the single crystals showed one sharp, isotropic line at any orientation of the magnetic field which means that there exists only one magnetically distinct site in the crystal. In both crystals, the g values are all different with two out of each set differing only by 0.03. Both of these observations are consistent with the proposed polymeric structure of a 2-substituted tetrazole (Fig. 1, bottom). The two g values which are almost equal correspond to the g values taken when the magnetic field is parallel to or perpendicular with the plane of the polymer. The proposed structure also has only one magnetically distinct site.

The g values may be used to make a rough calculation as to the amount of covalency in the copper-tetrazole bond. Assuming the structure at the bottom of Fig. 1 to be the structure of the complexes under consideration here, two formulae for the g values of an octahedral copper complex with a tetragonal distortion corresponding to elongation along a four-fold symmetry axis may be developed. The development

is similar to the development of the g value formulae derived in the introduction. The final formulae are:

$$g = 2.002 + \frac{8\xi}{\Delta_1} P$$

$$g = 2.002 + \frac{2\xi}{\Delta_2} P$$

ξ = the spin orbit constant for copper = 829 cm^{-1}

P = the one electron population of the copper d orbital [2]

Jonassen [5] reported the values for Δ_2 for both complexes but gave no value for Δ_1. With the above formulae, P may be calculated and then used to predict Δ_2. The results are given in Table 3.

Position and kind of substituent on tetrazole	Composition	g values	linewidths (gauss)
2-methyl-5 amino	$2(C_2H_5N_5)\ CuCl_2$	2.043 ± 0.002	24.5 ± 0.5
		2.073	29.4
		2.266	49.0
2-methyl-5 amino	$2(C_2H_5N_5)\ CuBr_2$	2.043 ± 0.002	22.0 ± 0.5
		2.073	34.3
		2.218	36.8

Now use $$P = \frac{(g_{11} - 2.002)\Delta_1}{8\xi} \qquad (1)$$

In the computation of $$\Delta_2 = \frac{2\xi P}{(g_1 - 2.002)} \qquad (2)$$

Chloride Complex	Bromide Complex
Given: $g_{11} = 2.266$	$g_{11} = 2.218$
$\Delta_1 = 14100\ cm^{-1}$	$\Delta_1 = 14380\ cm^{-1}$
Obtain from (1) P = 0.56	P = 0.47

Using these values of P and taking g_1 = average of g_{xx} and g_{yy}

= 2.058

Result: $\Delta_2 = 16580\ cm^{-1}$	$\Delta_2 = 13920\ cm^{-1}$

TABLE 3. RESULTS OF SINGLE CRYSTAL WORK

VII. THEORY OF THE ESR OF TRAPPED ORGANIC RADICALS

The effective spin Hamiltonian describing the interaction of the nuclei and electron of a trapped organic radical with the magnetic field and with one another has previously been written down in the section on the ESR of transition metals. It will be listed again to aid in the following discussion:

$$\mathcal{H} = \beta\vec{H} \cdot \vec{\vec{g}} \cdot \vec{S} - \sum_i \gamma_i \hbar \vec{H} \cdot \vec{I}_i + \sum_i \vec{S} \cdot \vec{\vec{A}} \cdot \vec{I}_i$$

In the section on transition metals, the first term of the effective spin Hamiltonian was thoroughly described. For trapped organic radicals, the g tensor of this term deviates only slightly from the free spin g value. It is symmetrical and its principal values are always close to the free spin g value. The second term represents the interaction of the nuclear spins with the magnetic field. The effect of this term is primarily to relax the selection rule $\Delta m_I = 0$.

Reference 10 contains an excellent description of the third term which represents the hyperfine interaction between the electron spin S and the nuclear spin I described by the second-rank tensor A. Insofar as g is nearly isotropic, the hyperfine tensor A will be a symmetrical 3 X 3 matrix which can be diagonalized and resolved into isotropic and anisotropic components. The effective Hamiltonian H' for the hyperfine interaction energy can be written:

$$\mathcal{H}' = \frac{8\pi g\beta\gamma}{3} \psi^2(0) \vec{S} \cdot \vec{I} - g\beta\gamma \left[\vec{S} \cdot \vec{I} r^{-3} - 3(\vec{S} \cdot \vec{r})(\vec{I} \cdot \vec{r}) r^{-5}\right].$$

The eigenvalues of H' are the principal values of A, and the isotropic and anisotropic components of A correlate with the first and second terms, respectively.

The first term in the equation for H' gives rise to a nonzero hyperfine splitting only if there is a finite probability of finding the unpaired electron at the interacting nucleus, as indicated by the factor $\psi^2(0)$. For this reason the isotropic interaction is usually called the contact or Fermi interaction. It is apparent that the isotropic hyperfine interaction A will only be nonzero if $\psi(o)$ is nonzero; that is, if the orbital of the unpaired electron has s-character.

The second term in the equation for H' imparts to the effective Hamiltonian an anisotropic or direction dependent character. This anisotropic part of the hyperfine tensor is a traceless tensor which describes the hyperfine interaction energy consequent upon the classical interaction of the electronic and nuclear dipoles.

In general, the hyperfine interaction of n nuclei of spin 1/2 will give rise to a spectrum consisting of 2^n equally intense lines. If two or more equivalent spin 1/2 nuclei interact, superposition of some of the lines results in a spectrum of n + 1 lines of binomial intensity distribution.

VIII. BACKGROUND ON THE ESR SPECTRA OF TRAPPED ORGANIC RADICALS

A considerable amount of work has been done on the subject of the ESR spectra of radiation damaged organic crystals. Naturally, the work has covered those materials from which single crystals are easily obtained. Crystals of saturated carboxylic acids and their salts, the simpler amino acids and certain unsaturated acids, when irradiated with x-rays, gamma rays, or high energy electrons, have been found to provide suitable hosts for the trapped radicals produced by such irradiation. Analysis of the spectra from radiation damaged crystals of these materials is primarily concerned with the identification of the trapped radical(s) via the interpretation of the proton hyperfine interaction. One type of radical which is commonly detected is a π - electron radical centered on a carbon atom. In such a radical the unpaired electron predominantly occupies a carbon 2p orbital perpendicular to the plane of the radical.

Kispert and Rogers [13] reported the interpretation of the ESR spectrum of single crystals of sodium acetate trihydrate irradiated with 1 Mev electrons at 77° K. At this temperature, they observed a four line pattern with intensity ratio of 1:3:3:1 and proton hyperfine splitting of 22.5 gauss. Each of these lines had two satellites spaced 5.6 gauss on either side to form a twelve line pattern. They interpreted the main four line pattern to be due to the methyl radical, $\cdot CH_3$. The satellite lines were attributed to spin flip transitions arising from a simultaneous change in the spin state of the odd electron on the methyl radical and of the neighboring protons of the molecules of water of crystallization. One of the first workers to

investigate the ESR of an x-irradiated single crystal of methyl malonic acid was Heller [14]. He irradiated the malonic acid at room temperature and observed the spectra at room temperature, 77°K, and 4° K. Heller interpreted his spectra in terms of the two species $CH_3\dot{C}(COOH)_2$ and $CH_3\dot{C}HCOOH$. He concentrated his efforts on the first and concluded, from the spectra, that the three methyl protons are equivalent, and the principal values of their hyperfine coupling tensor are 75.4 (along the $C\text{-}CH_3$ bond), 68.8 and 68.6. He also concluded that the isotropic component of the coupling tensor (and, therefore, the spin density on the methyl protons) is positive, and that the methyl group executes nearly free rotation about the C-C bond at 4.2° K. Tamura, Collins, and Whiffen [15] irradiated various malonic acids at 77° K and observed the ESR spectra as the temperature was raised. They found that the radical formed at 77° K was of the form $R\text{-}CH_2\text{-}\dot{C}H(COOH)$, and that as the temperature was raised, a reaction took place in which the original radical disappeared and a radical of the form $RCH_2\dot{C}(COOH)_2$ showed up in its place.

J. R. Morton [16] reported the ESR spectrum of $(CH_3)_2CO_2^-$ trapped in α-aminoisobutyric acid at 40° K. He concluded that at this temperature, one of the methyl groups is undergoing virtually free rotation about the $C\text{-}CH_3$ bond, while the other methyl group is undergoing hindered rotation. Box and Freund [17] investigated x-irradiated α-aminoisobutyric acid irradiated at 77°K. They allowed the crystal to warm gradually and observed the resulting spectra. They detected distinct intermediate ESR spectra due to preliminary conformations of the radical present at room temperature. They found the intermediate spectra to be better resolved and easier to interpret than the final spectrum.

They also found that cooling the intermediate fragment to 77° K showed no change in the spectrum, but that cooling the room temperature fragment did show a changing spectrum. They interpreted this behavior as resulting from different conformations of $(CH_3)_2\dot{C}COOH$.

Miyagawa and Gordy [18] first reported the results of their investigation of room temperature irradiated single crystals of alanine. They proved that the stable free radical produced by the irradiation was of the form $CH_3\dot{C}HR$, where R is a group which has no nuclei with detectable coupling. The hydrogens of the methyl group of the radical were shown to have equivalent, isotropic coupling of 26 gauss each, essentially independent of the frequency of observation. Horsfield, Morton, and Whiffen [19 and 20] observed the change in the ESR spectrum of the room temperature gamma irradiated single crystal of l-α-alanine on cooling to 77° K, and interpreted their results in terms of the cessation of rotation of the methyl group of the trapped radical $CH_3\dot{C}HCOOH$. The isotropic hyperfine couplings of the three hydrogens of the methyl group were found to be 120, 76, and 14 Mc/sec compared to the value of 70 Mc/sec each at 300° K. In the intermediate temperature range between 100° K and 200° K, the spectra were found to differ from the spectra above and below these temperatures. From the line width change near 100° K and 200° K, an estimate of approximately 4 kcals/mole was made for the activation energy hindering the rotation of the methyl group. Miyagawa and Itoh [21] determined that room temperature gamma irradiated single crystlas of dl-alanine grown from heavy water exhibited the same hyperfine structure as those crystals grown from normal water except that the line widths were considerably sharper. They observed the spectra as the temperature was lowered and concluded that

the rotation of the methyl group was hindered at lower temperatures. They used a modified Bloch equation to estimate the frequency of rotation of the methyl group from the absorption patterns at various temperatures, and by applying the classical theory of rate processes to analyse the relation between the frequency of rotation and the temperature, they found the potential barrier to internal rotation of the methyl group to be 3.6 kcal/mole.

Sinclair and Hanna [22 and 23] examined the ESR spectra of l-alanine-1-^{13}C, x-irradiated at 80° K. They concluded that the low temperature initial species has a high unpaired electron population on the carboxyl carbon and that as the low temperature radical is allowed to decay thermally to the fragment $CH_3\dot{C}HCOOH$ at 140-150° K, there is a transfer of the unpaired electron from the carboxyl group to the α-carbon. The $CH_3\dot{C}HCOOH$ is at a different orientation in the crystal than the $CH_2\dot{C}HCOOH$ formed by irradiation at room temperature. Upon warming to room temperature, a reorientation of the fragment occured which gave the usual room temperature ESR spectrum. A feature of the intermediate fragment was that the methyl protons remained equivalent even when re-cooled to 80° K. This was in contrast to the room temperature fragment where the rapid interconversion of methyl protons was frozen out by cooling to 77° K.

Wells and Box [24] studied the rotation of the methyl group in the free radical $C\ell CH_2$-CONH-C(CH_3)COOH by ESR and ENDOR spectroscopy. They analyzed their results using a quantum mechanical hindered rotor model with Mathieu functions as basis functions. Their experimental results indicated a barrier height of less than 0.5 kcal/mole for the methyl group rotation.

In recent paper on x-irradiated single crystals of zinc acetate dihydrate, Tolles, Crawford, and Valenti [25] reported the presence of the methyl radical in the case of irradiation at 77° K, with the subsequent disappearance of this radical and the appearance of $\cdot CH_2CO_2^-$ as the temperature was raised. They proposed a mechanism to explain the decay of the first species and corresponding increase in the second species. The mechanism involves abstraction of a hydrogen atom by the methyl radical from a neighboring acetate ion. They supported this hypothesis by synthesizing $Zn(CH_2DCO_2)_2 \cdot 2H_2O$ and showed that the decay and growth of the above species exhibits an isotope effect. Spectra taken over a range of temperatures revealed both the slow and rapid exchange of the hydrogen atoms seen previously [e.g. 16,17,18], with the barrier to internal rotation of the $-CH_2$ group being 5 kcal/mole.

IX. EXPERIMENTAL WORK

A. GROWING OF CRYSTALS

Single crystals of strontium acetate hemihydrate were grown by slow evaporation from a saturated aqueous solution at room temperature. Crystals in which heavy water was exchanged for the water of hydration were grown by making a saturated solution of the strontium acetate hemihydrate in 99% D_2O at room temperature, and then allowing slow evaporation of the solution. The single crystals crystallized in the form shown in Fig. 5 which enabled definition of an orthogonal crystal axis system. The crystals cleave easily parallel to the XY plane. The XYZ crystal axis system is shown in Fig. 5. The numbers along the edges of the crystal are the angles the crystal faces make with the XY plane.

B. IRRADIATION OF THE CRYSTAL

The single crystals were exposed to x-irradiation at 50 KV and 40 ma from a copper target. The crystals irradiated at room temperature were placed on scotch tape and mounted in the open windows of the x-ray machine allowing the port covers to be closed at all times. For room temperature irradiations, the crystals were exposed for one hour. For irradiation at liquid nitrogen temperature, the crystals were placed in a quartz tube sealed at one end. The other end was stoppered to prevent condensation of liquid air into the tube. The tube with crystals was placed in a styrofoam ice bucket and precooled gradually by slowly pouring liquid nitrogen into the bucket and allowing the cold gas to flow over the tube. Precooling was necessary to prevent shattering of

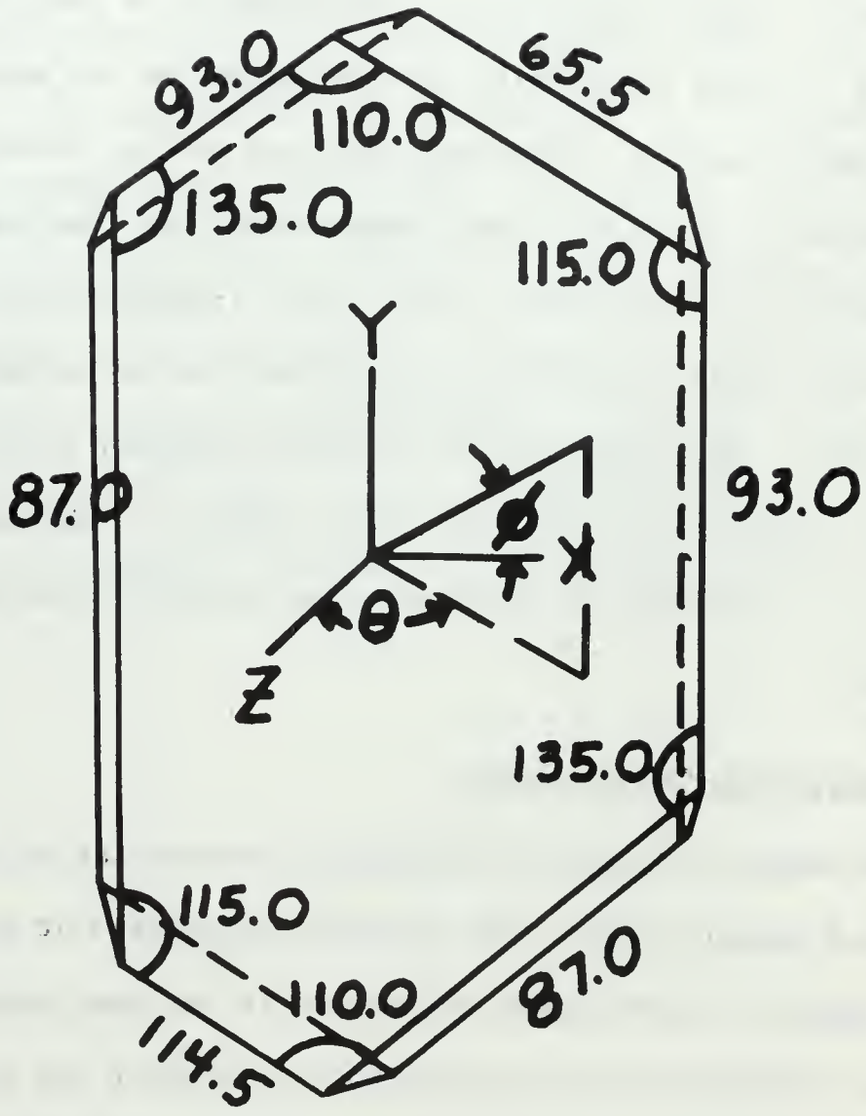

FIGURE 5. A single crystal of $Sr(CH_3CO_2)_2 \cdot \frac{1}{2}H_2O$ showing the angles between the edges and faces of the crystal, and the orthogonal crystal axis system.

the crystal when exposed to a sudden temperature change. Eventually, the tube was immersed completely in liquid nitrogen. The bucket was mounted on a ring stand with a lead shield attached, and a wooden cover with a hole drilled in the top of the bucket. The bucket was placed in front of the x-ray port, and the tube positioned in the x-ray beam so that the crystal received maximum dosage for a two hour period. The position of the tube in the beam was checked by darkening the room and lowering a piece of fluorescent paper into the bucket. The tube and crystal formed a shadow on the fluorescent paper.

C. CRYSTAL ALIGNMENT

The orientation of the crystal in the spectrometer cavity had to be determined as precisely as possible in order to determine the location of the magnetic field with respect to the crystal axis system. The crystal was mounted on a quartz rod which had two flats ground parallel to each other on both ends of the rod. The crystal was held on the rod by means of a platinum spring attached to the rod by a piece of scotch tape. The end opposite the mounted crystal was clipped to an angle indicator positioned over the center of the spectrometer cavity. The crystal was positioned on the rod by use of a microscope, one of the eyepieces of which had crosshairs. The orientations of the crystal on the rod were chosen so that the well defined edges of crystal were parallel or perpendicular to the edges of the rod. The angles between the faces and edges of the crystal were determined with an optical goniometer. For liquid nitrogen work, the crystal alignment was accomplished without warmup of the crystal by keeping the crystal immersed in a bath of liquid nitrogen under the microscope.

D. TAKING THE SPECTRA

The spectra were taken with the spectrometer previously described for the liquid nitrogen work on copper tetrazole. The temperature was controlled with the temperature control unit attachment to the spectrometer used for the copper tetrazole work.

X. RESULTS

A. ROOM TEMPERATURE SPECIES

Spectra obtained from x-ray damaged single crystals of strontium acetate hemihydrate at room temperature were found to depend upon the history of the crystal as well as the orientation of the magnetic field relative to the crystal axis system. As can be seen in Fig. 6 (top), crystals irradiated at liquid nitrogen temperature, slowly warmed to room temperature, and then observed at room temperature did not exhibit the extra central line in the spectrum as did the crystals irradiated and observed at room temperature (Fig. 6, bottom). Both spectra were obtained at the same crystal orientation of $\phi = 0^{\circ}$, $\theta = 90^{\circ}$. Reorientation of the magnetic field resulted in a coalescence of the two 1:3:3:1 patterns into what appears to be a 1:4:6:4:1 pattern as in Fig. 7. The orientations for the magnetic field are from top to bottom, respectively $\phi = 0^{\circ}$, $\theta = 45^{\circ}$; $\phi = 0^{\circ}$, $\theta = 80^{\circ}$; $\phi = 0^{\circ}$, $\theta = 90^{\circ}$. The spectra can be interpreted in terms of a free radical species with three equivalent hydrogens split by a fourth, inequivalent hydrogen. The spectra obtained also indicate that there is only one magnetically distinct site in the crystal for the room temperature species.

For some orientations of the magnetic field, the base line of the spectrum was not straight, but rather convex upward. The sweep range was therefore changed from 250 gauss to 1000 gauss and the spectra in Fig. 8 were obtained. The spectra indicate the possible presence of a triplet.

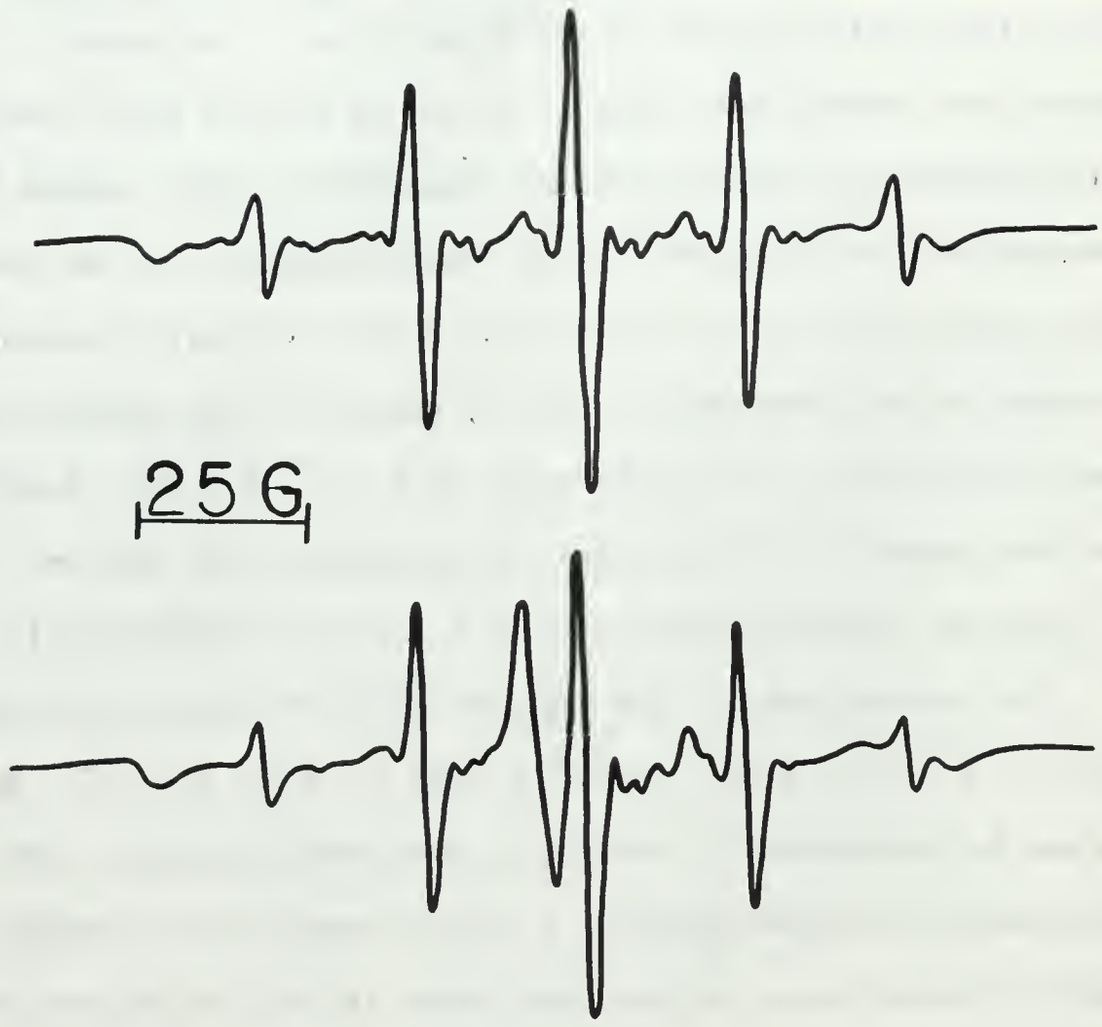

FIGURE 6

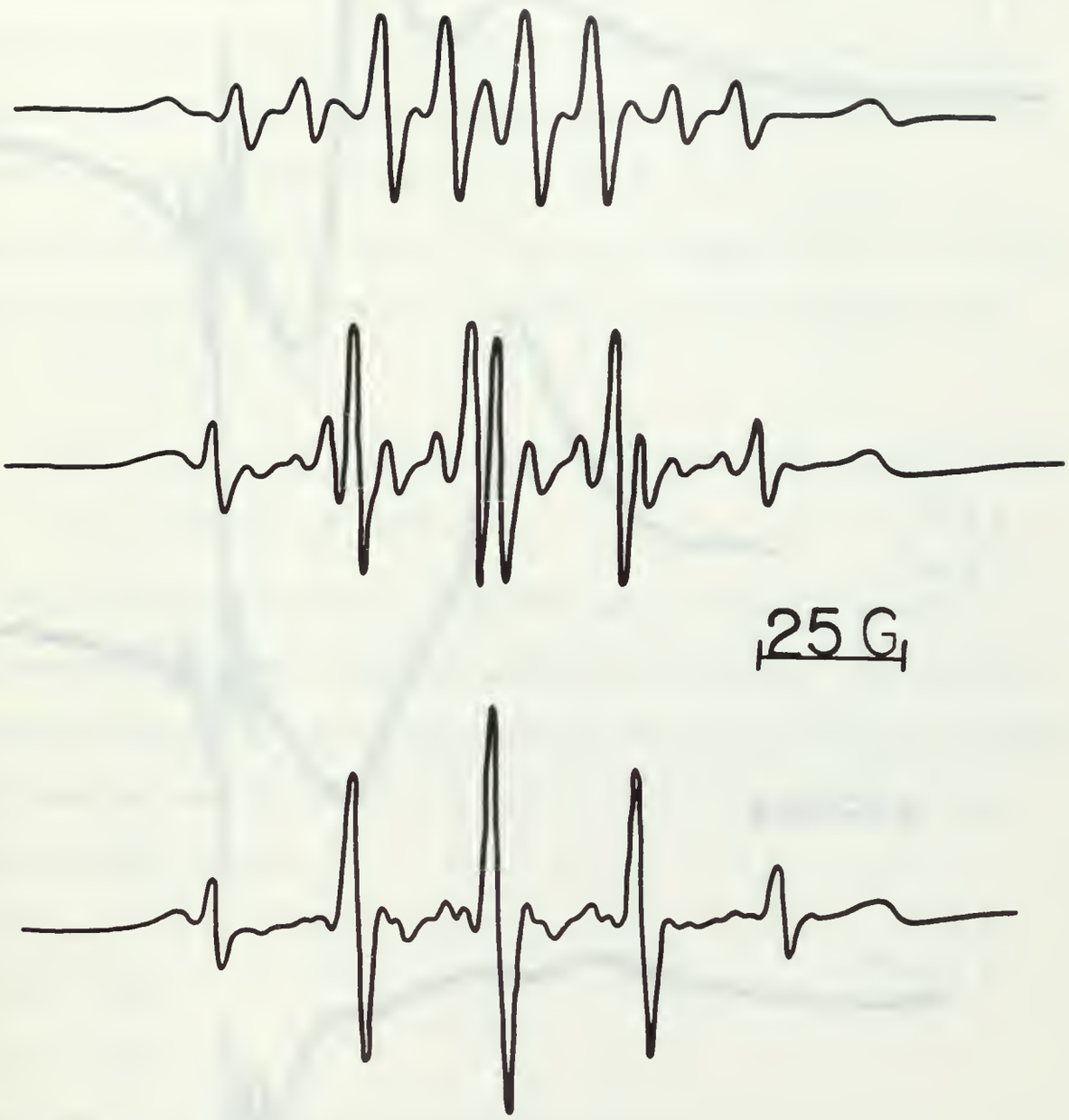

FIGURE 7

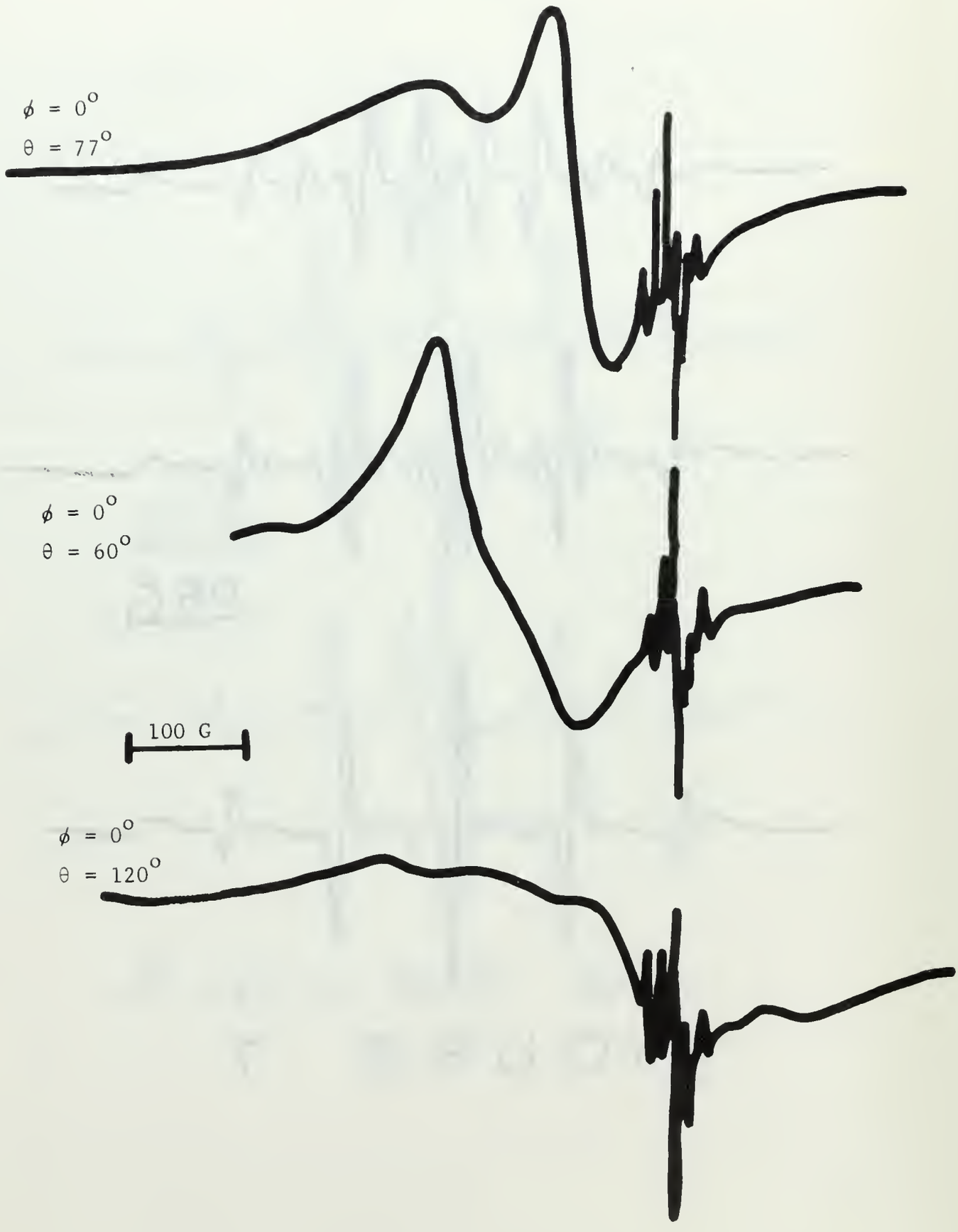

FIGURE 8. Broad line species seen in $Sr(CH_3CO_2)_2 \cdot \frac{1}{2} H_2O$ irradiated and observed at room temperature.

Several spectra of the room temperature species were taken at different magnetic field orientations. The coupling constant for the inequivalent hydrogen was not always obtainable due to the overlapping of the spectral lines at several orientations. However, the coupling constant for the CH_3 group was always obtainable. The methyl group coupling constants and corresponding magnetic field orientations were plotted on a stereographic net, and an estimate of the positions of the principal axis system and the coupling constants along the principal axis was made, assuming axial symmetry for the rotating methyl group. The results are:

A_{11} = 27.1 $\pm$ 0.4 gauss, direction cosines (-0.32, 0.38,-0.87)

$A_{\perp}$ = 24.2 $\pm$ 0.4 gauss

The errors in the direction of the principal axis are estimated to be ten degrees and for the coupling constants, 0.5 gauss. The coupling constants and magnetic field orientations for the inequivalent hydrogen were least squared [26]. The results are, for the three principal values of the A tensor:

(a) 11.61 $\pm$ 0.40 gauss

(b) 32.98

(c) 19.32

The direction cosines for the principal axes are:

(a) (0.72, 0.69, 0.80)

(b) (-0.18, 0.73, 0.98)

(c) (0.67, -0.72, 0.18)

in the XYZ axis system in Fig. 5. The data used is in Table 4. Figure 9 shows the angular dependence of the coupling constant. The graphs indicate that the methyl group coupling constants show a cosθ dependence.

ϕ	θ	a^{CH_3} (gauss)
0	25	25.54 ± 0.35
	30	25.24
	35	25.24
	40	25.06
	45	24.90
	50	24.56
	55	24.56
	60	24.38
	65	24.38
	70	24.20
	80	24.38
70	30	25.58
	45	24.90
	60	24.38
	75	24.38
	90	24.20
	105	24.90
	120	25.41
	135	26.28
	150	26.45
45	0	26.10
	15	25.93
	30	25.54
	45	25.24

TABLE 4. Coupling constants and magnetic field orientations for the room temperature species.

Table 4 continued.

ϕ	θ	a^{CH_3} (gauss)
(45)	60	24.55 ± 0.35
	75	24.38
	90	24.20
	105	24.20
	120	25.24
	135	25.76
	150	26.28
90	0	26.28
	15	25.93
	30	25.24
	45	25.06
	60	24.90
	75	24.38
	90	24.55
	105	25.06
	120	25.59
	135	26.10
	150	26.45
	165	26.23
25	30	25.42
	45	24.72
	60	24.38
	75	24.38
	90	24.20
	105	25.06
	120	25.42
	135	26.28
	150	26.45
	165	26.80

Table 4 continued.

ϕ	θ	a^{CH_3} (gauss)
115	0	25.93 ± 0.35
	15	25.93
	30	25.54
	45	25.06
	60	24.38
	75	24.77
	90	24.56
	105	24.90
	120	25.93
	135	26.45
	150	26.97
	165	26.62

ϕ	θ	a^{H} (gauss)
0	25	17.12 ± 0.35
	30	15.04
	35	13.83
	40	12.10
	45	11.24
	50	11.06
	55	11.93
	60	13.83
	65	15.73
	70	16.94
25	30	15.22
	45	10.54
	60	12.44
	75	17.29
	120	29.39
	135	30.60
	150	30.26

Table 4 continued.

ϕ	θ	a^H (gauss)
45	15	20.74 $\pm$ 0.35
	30	16.94
	45	13.31
	60	12.80
	75	15.90
	90	20.22
70	30	20.22
	45	18.15
	60	16.94
	75	17.46
	90	14.01

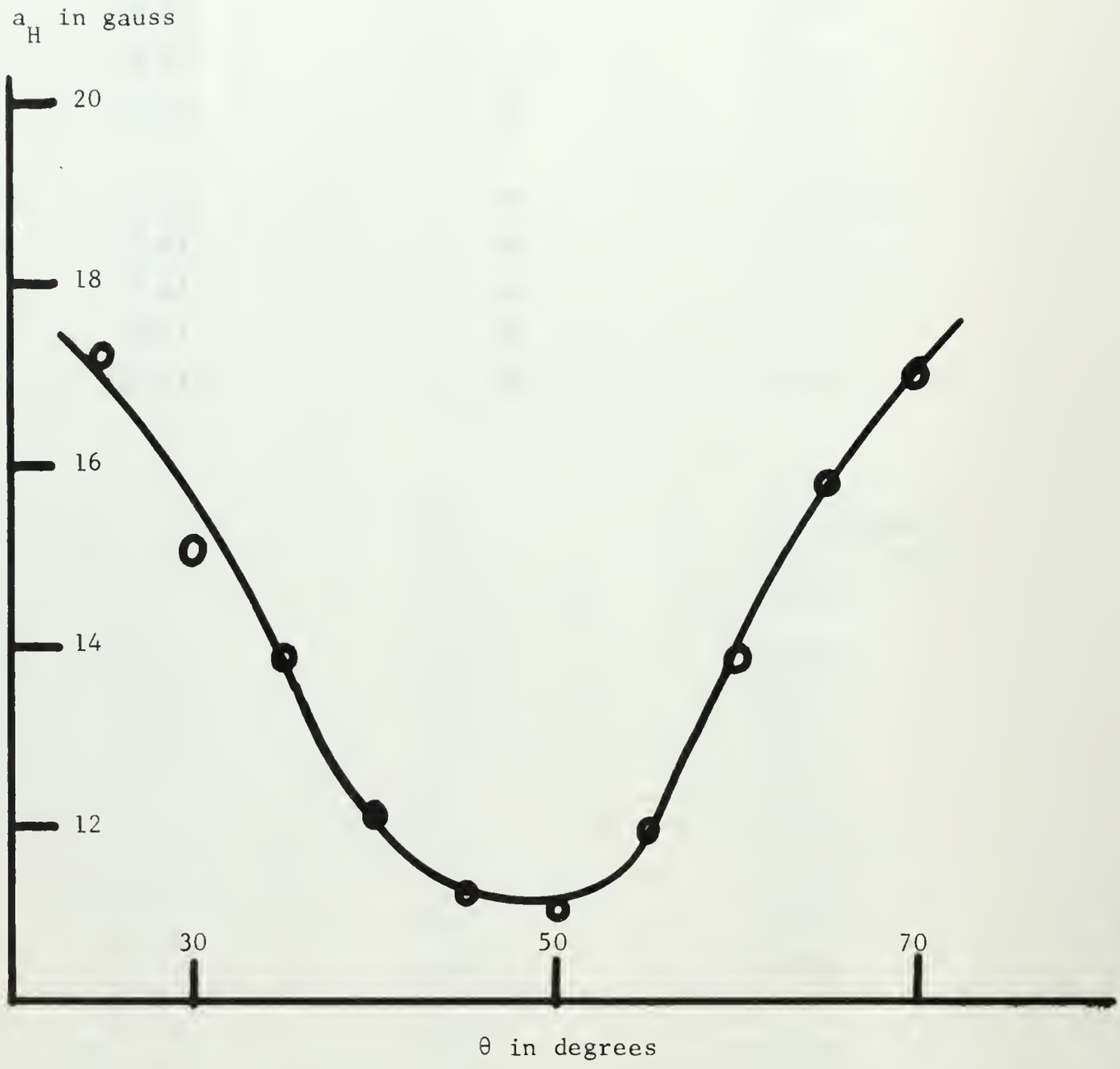

FIGURE 9A. H atom coupling constant versus orientation of magnetic field in XYZ axis system. $\emptyset = 0^o$

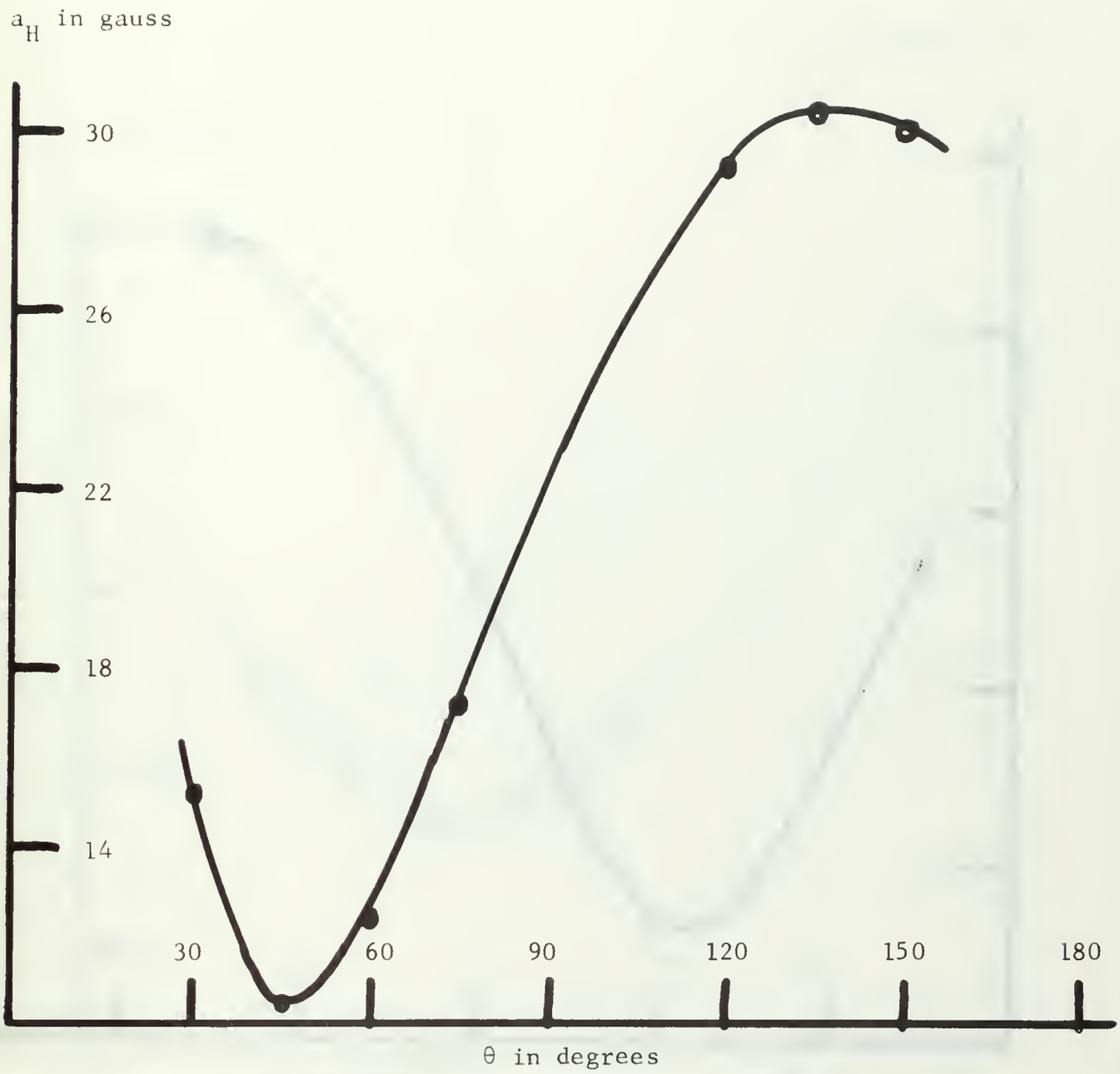

FIGURE 9B. $\phi = 25^{\circ}$

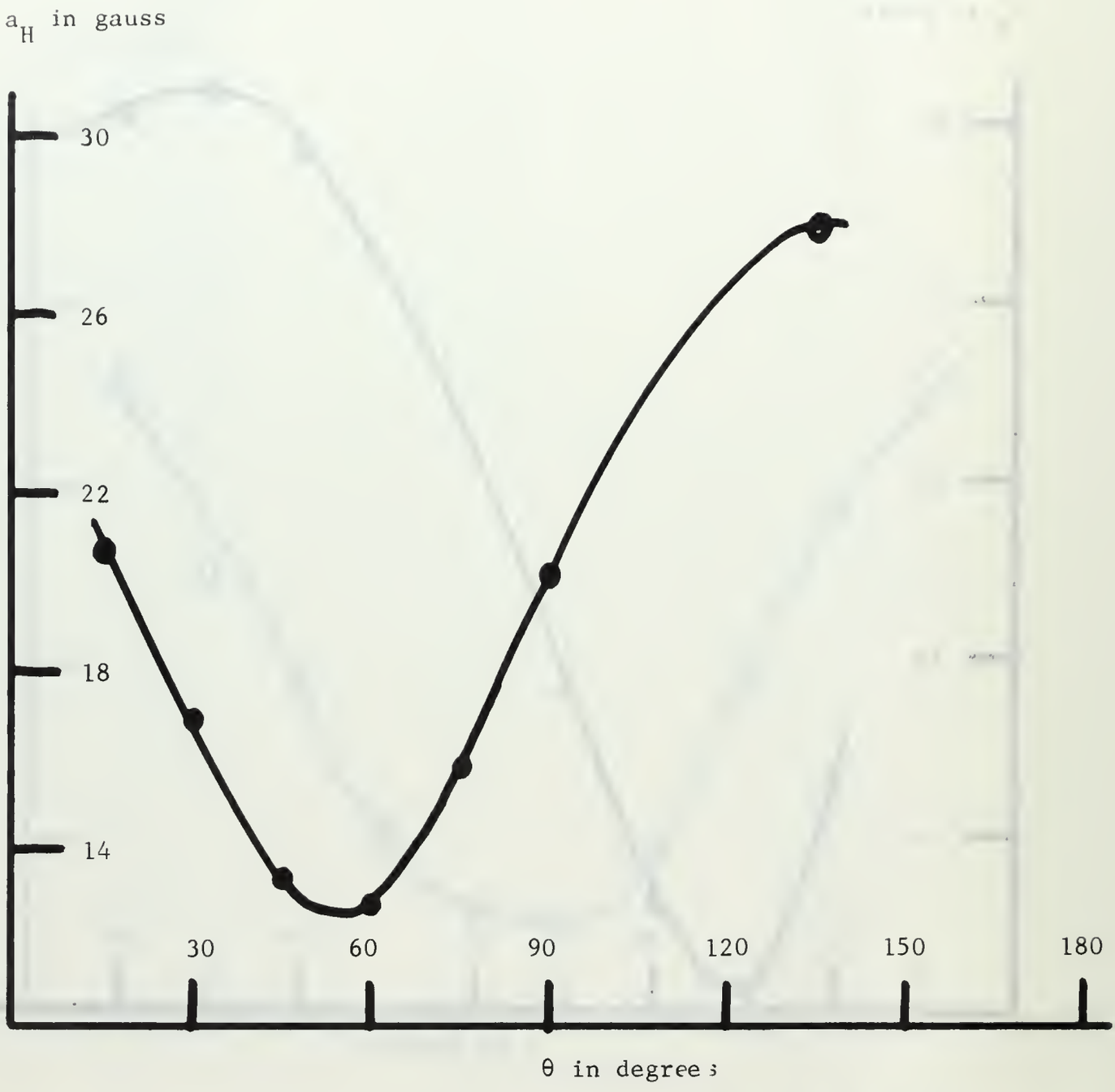

FIGURE 9C. $\phi = 45^{\circ}$

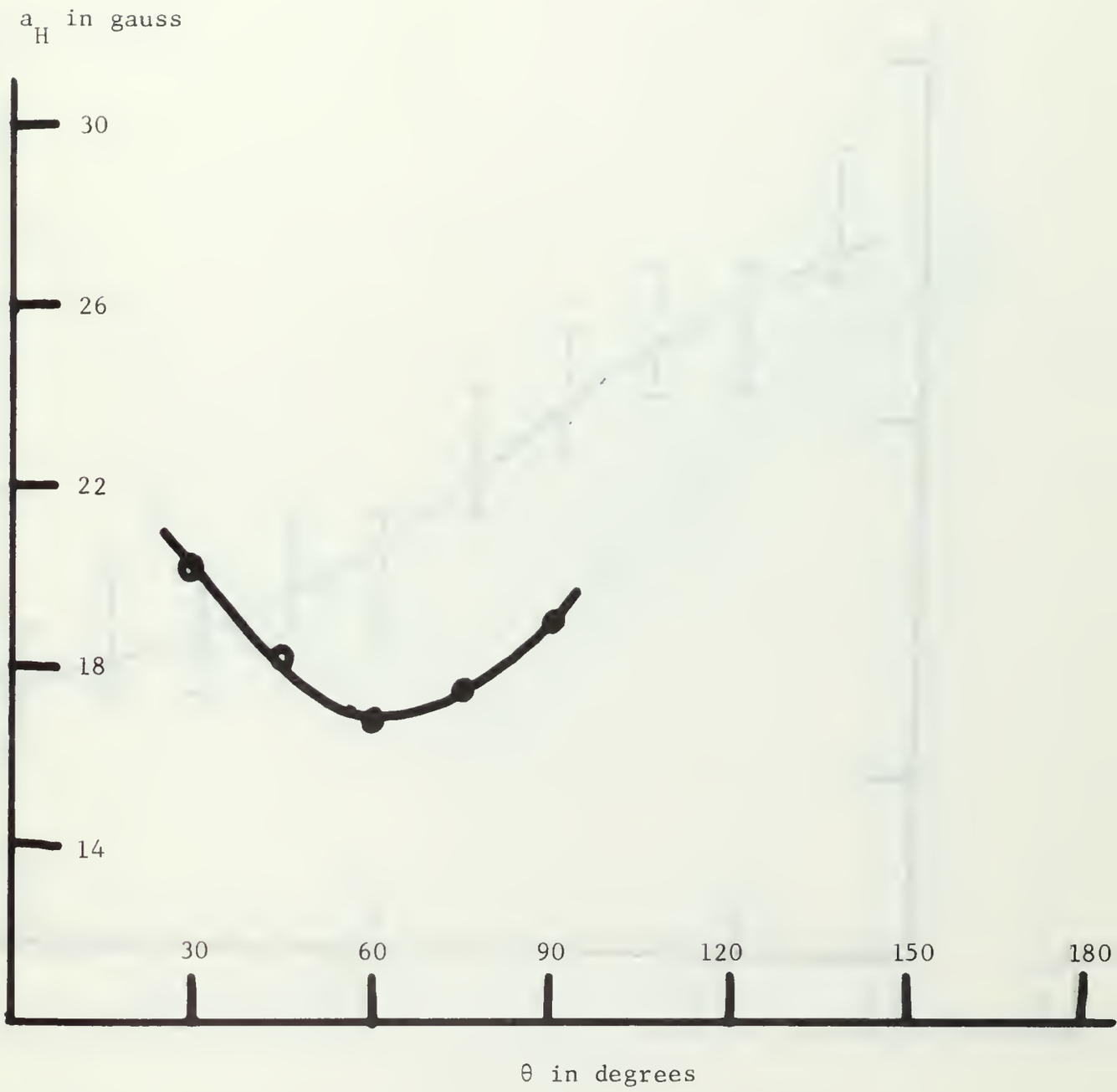

FIGURE 9D. $\phi = 70^{\circ}$

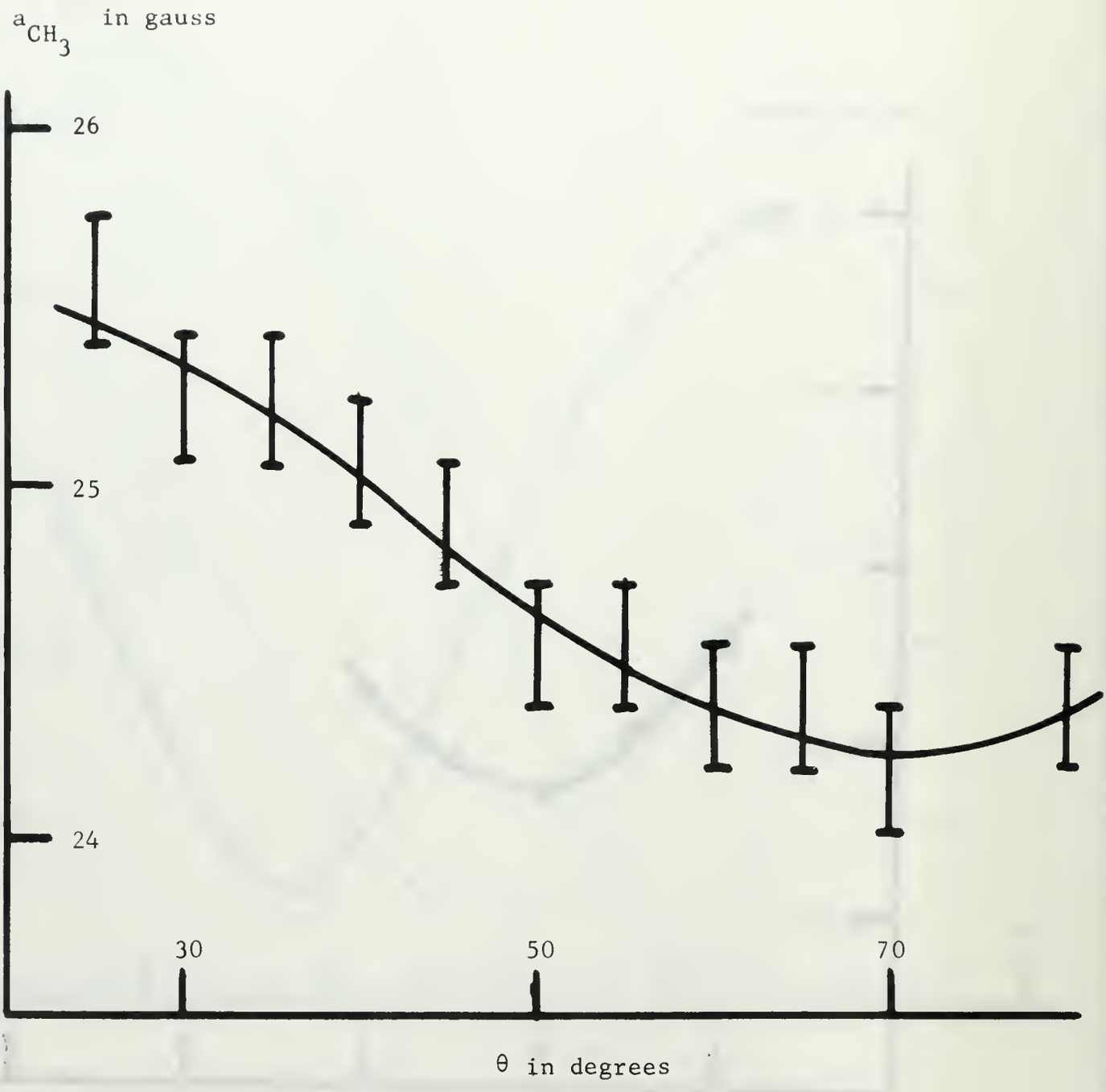

FIGURE 9E. CH_3 group coupling constant versus orientation of magnetic field in XYZ axis system. $\phi = 0^o$

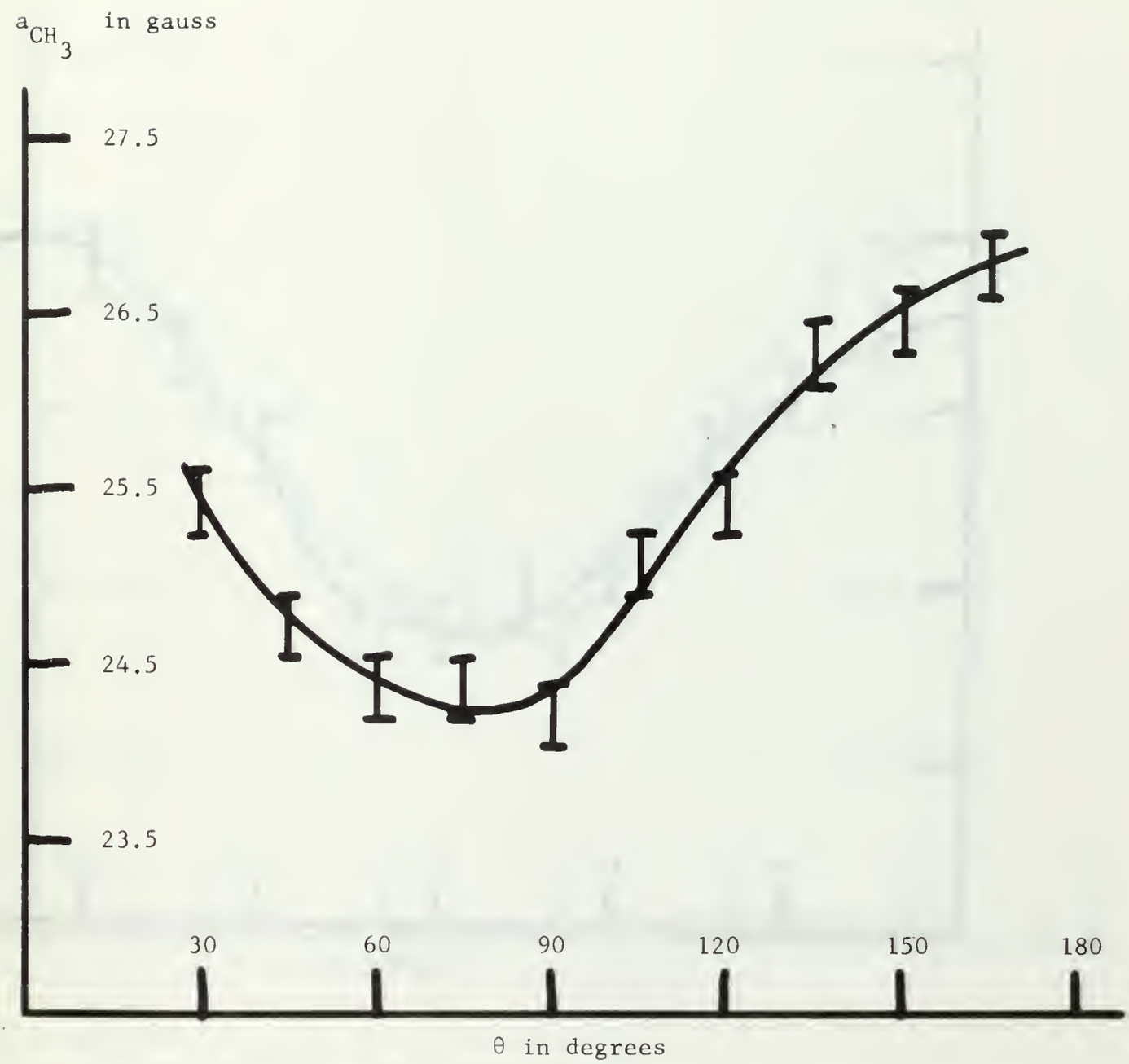

FIGURE 9F. $\phi = 25^{\circ}$

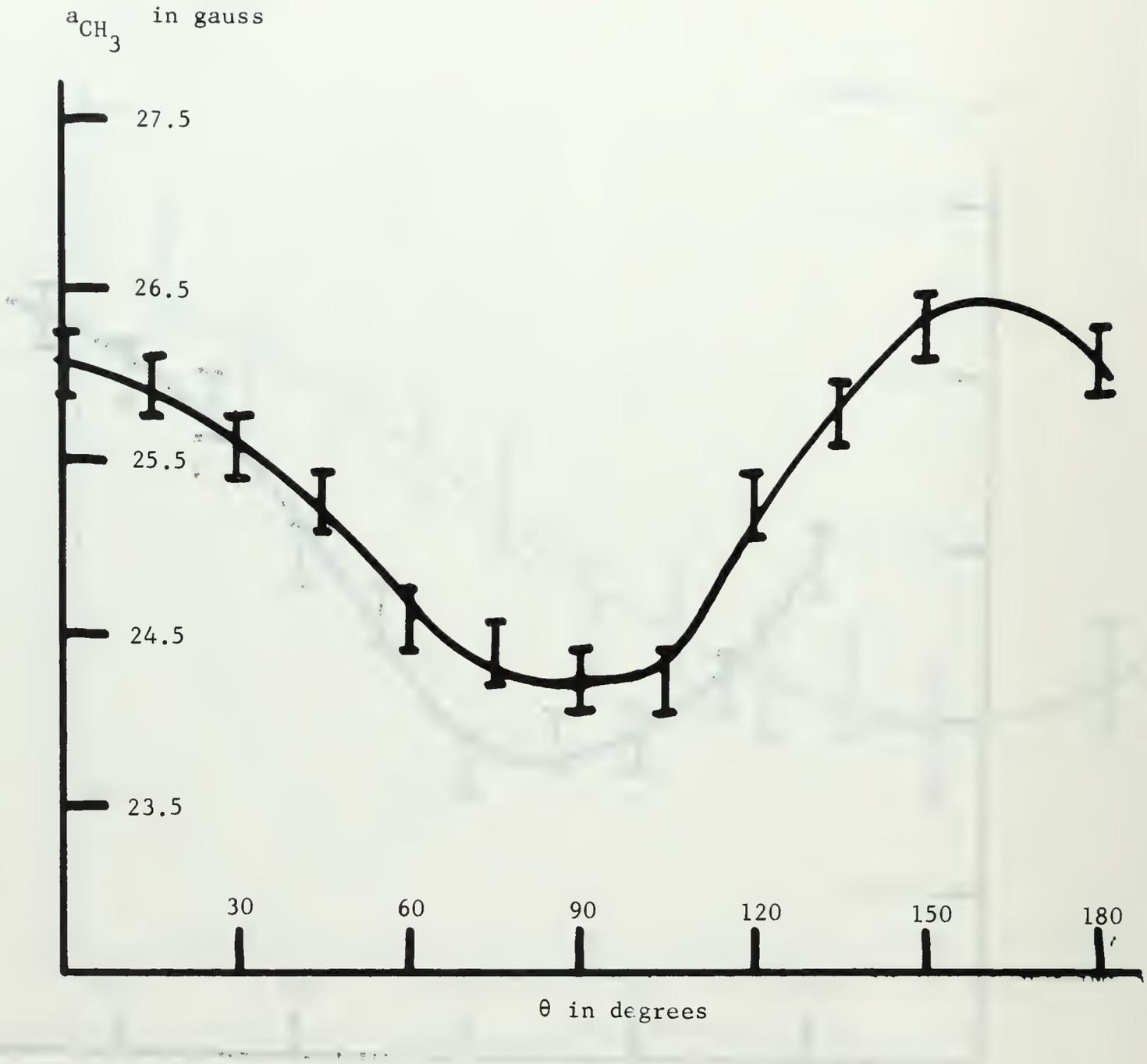

FIGURE 9G. $\phi = 45^{\circ}$

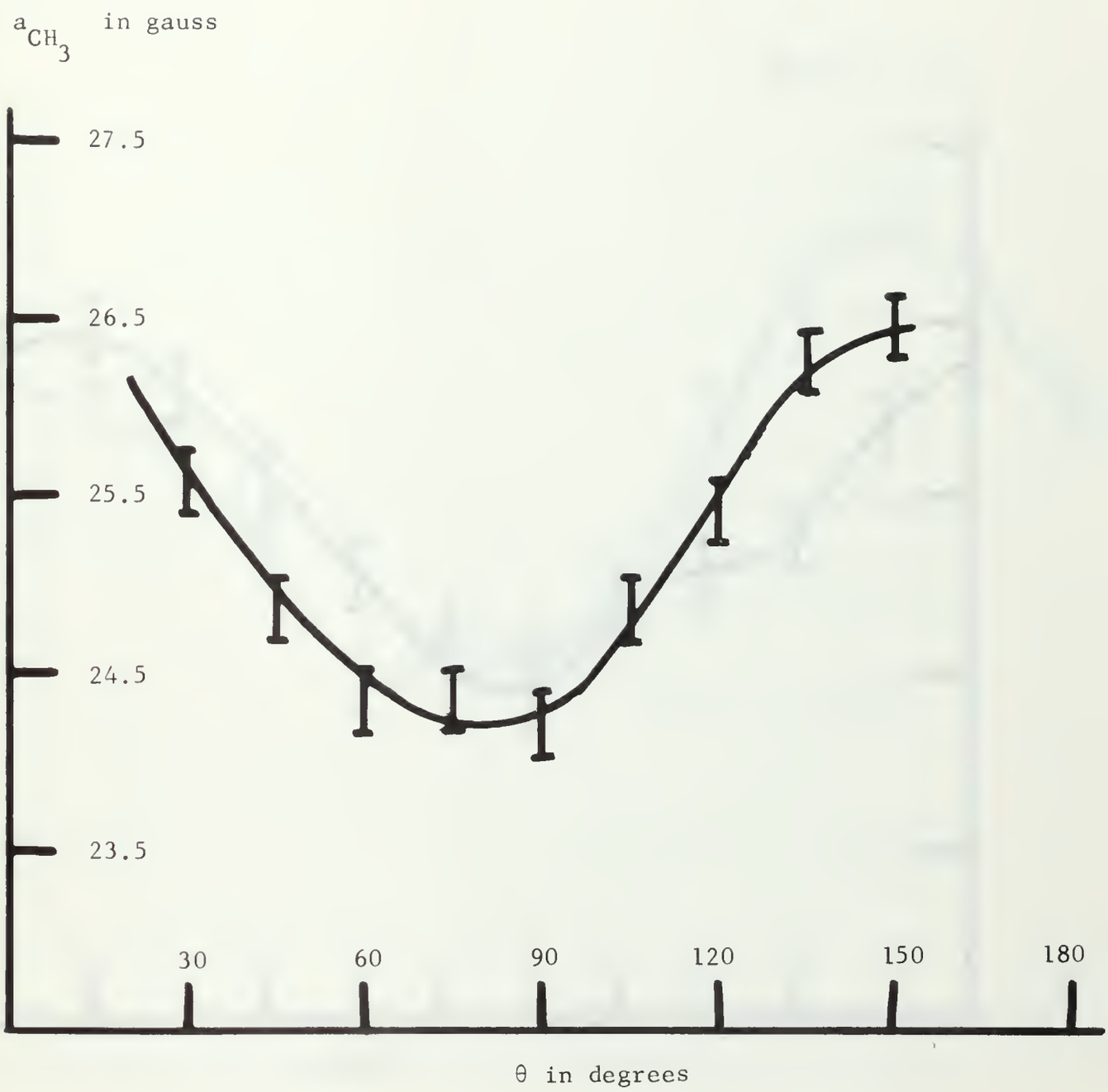

FIGURE 9H. $\phi = 70^{\circ}$

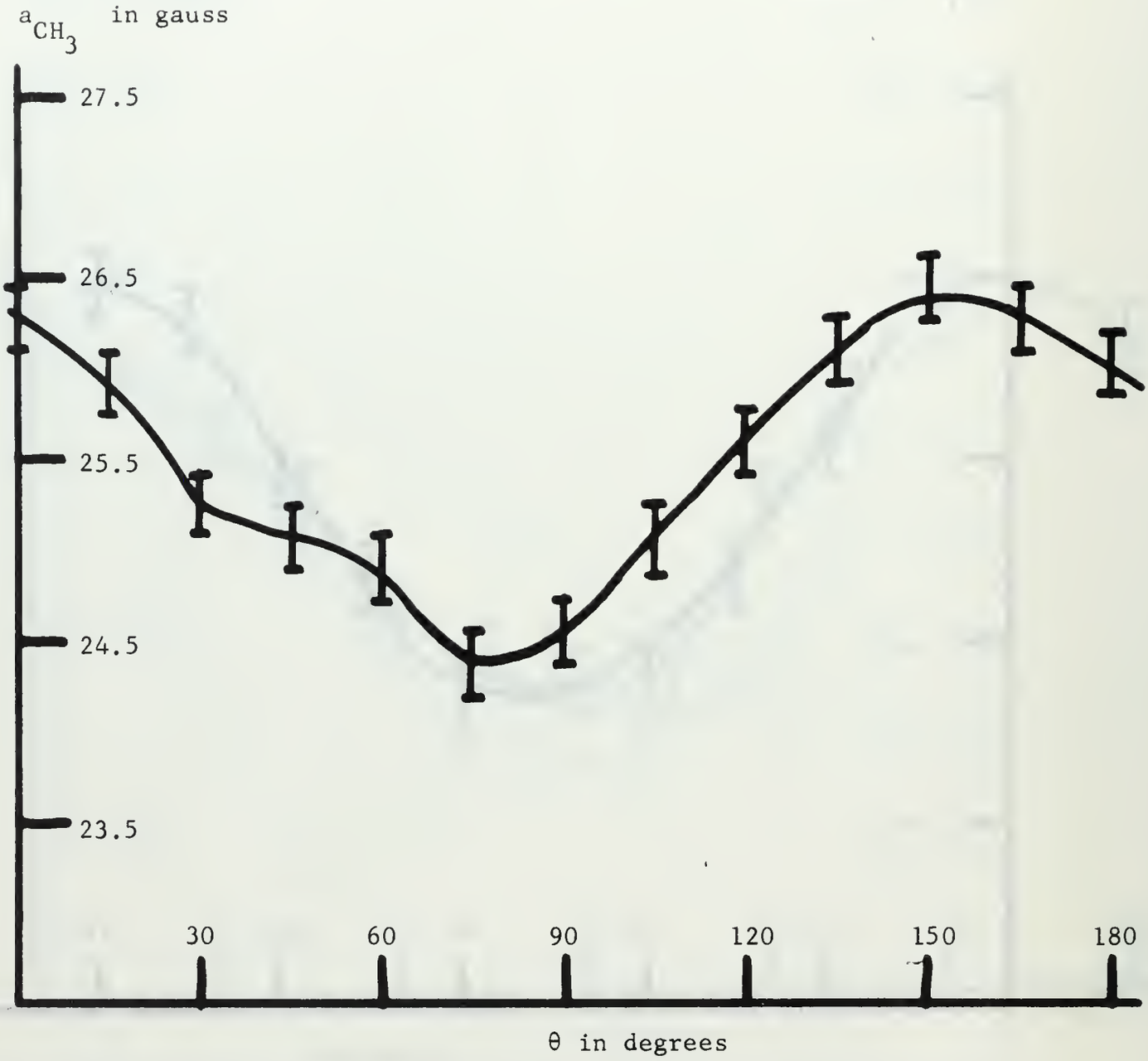

FIGURE 9I. $\phi = 90^{o}$

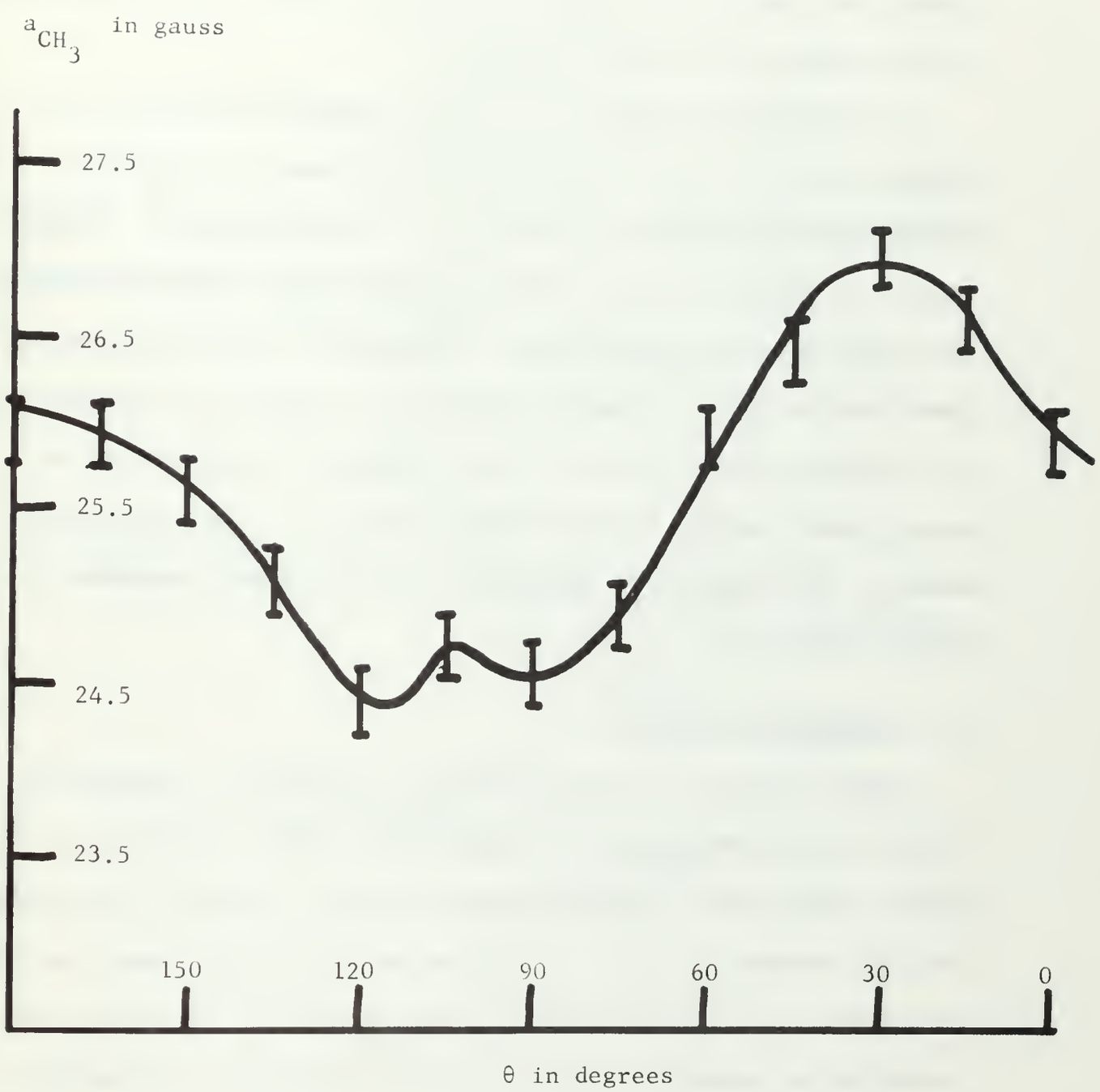

FIGURE 9J. $\phi = 115^{o}$

Powdered strontium acetate hemihydrate was recrystallized from 99% D_2O and the resulting radiation damaged crystals showed the same spectrum as single crystals recrystallized from normal water. It may be concluded that the water of hydration does not enter into reactions involving the initial free radical fragments.

An interesting sidelight to the room temperature work is that a crystal of zinc acetate dihydrate which had been x-ray damaged and then set aside for one month was looked at on the spectrometer. Surprisingly, the spectrum obtained was the same 1:4:6:4:1 pattern obtained for strontium acetate hemihydrate. Apparently, the radical species identified by Tolles, Crawford, and Valenti [25] was an intermediate in a reaction with a very small rate constant or large activation energy which leads to a final product similar to that in strontium acetate. The spectrum of the species in zinc acetate dihydrate is shown in Fig. 10.

B. INTERMEDIATE SPECIES

Single crystals of strontium acetate hemihydrate irradiated at liquid nitrogen temperature and observed at -100° C exhibited a 1:3:3:1 pattern which split into eight lines of equal intensity as the temperature was lowered to -160° C. Spectra for the species present at -100°C were taken over several orientations of the magnetic field, the coupling constants and magnetic field orientations plotted on a stereographic net, and, assuming axial symmetry for a rotating methyl group, the hyperfine coupling constants and direction cosines of the species relative to the XYZ axis system in Fig. 5 were calculated to be [26]:

A_{11} = 12.84 $\pm$ 0.30 gauss

$A_{\perp}$ = 10.04 $\pm$ 0.30 gauss

X = (0.81, 0.58, 0.06)

Y = (-0.59, 0.80, 0.12)

Z = (0.02, -0.14, 0.99)

The data fed into the program is in Table 5. The average isotropic hyperfine coupling constant is 9.2 gauss.

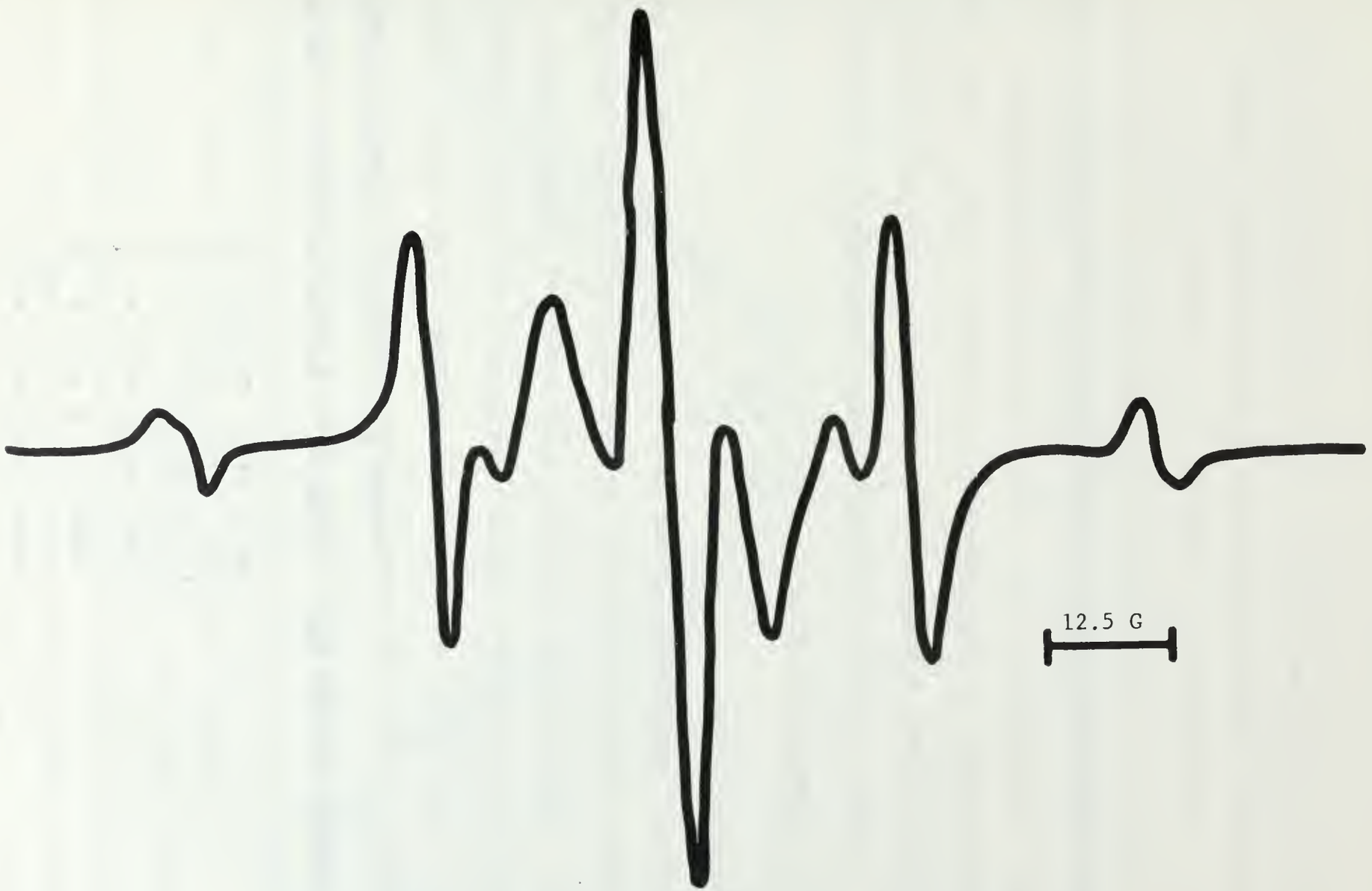

FIGURE 10. Spectrum of one month old x-ray damaged single crystal of $Zn(CH_3CO_2)_2 \cdot 2H_2O$

ϕ	θ	a^{CH_3}(Mc/sec)
0	0	35.89 $\pm$ 1.00
	20	36.83
	40	36.27
	60	32.16
	70	31.78
	80	30.28
	90	29.35
	100	27.86
	110	28.60
	120	28.42
	140	31.03
	160	33.84
90	0	35.33
	20	36.36
	40	34.96
	60	31.03
	70	29.16
	80	28.42
	90	27.86
	100	27.29
	110	28.04
	120	28.98
	140	31.22
	160	34.21

TABLE 5. Coupling constants and magnetic field orientations for the -100^{o} C species.

Table 5 continued

ϕ	θ	a^{CH_3} (Mc/sec)
45	0	35.71 $\pm$ 0.35
	20	34.40
	40	31.41
	60	28.79
	80	27.48
	90	27.11
	100	28.60
	110	29.72
	120	31.59
	140	33.46
	160	35.33
135	0	35.71
	20	36.64
	40	35.33
	60	33.28
	70	30.10
	80	29.54
	90	28.23
	100	28.04
	110	27.86
	120	28.60
	140	28.60
	160	32.90

The spectra of this same species were obtained as a function of temperature. The computer program following the appendix, which is based upon the mathematical model for motional and exchange narrowing of spectral lines, was used to predict the spectrum of the rotating methyl group for various rotational frequencies. In the drawing below, the eight line pattern resulting from splitting by three equivalent protons corresponds to the zero rotation case. In the case of rotation of the methyl group, all of the lines except the two outside lines exchange, and the extent to which they exchange is a function of the frequency at which the methyl group is rotating:

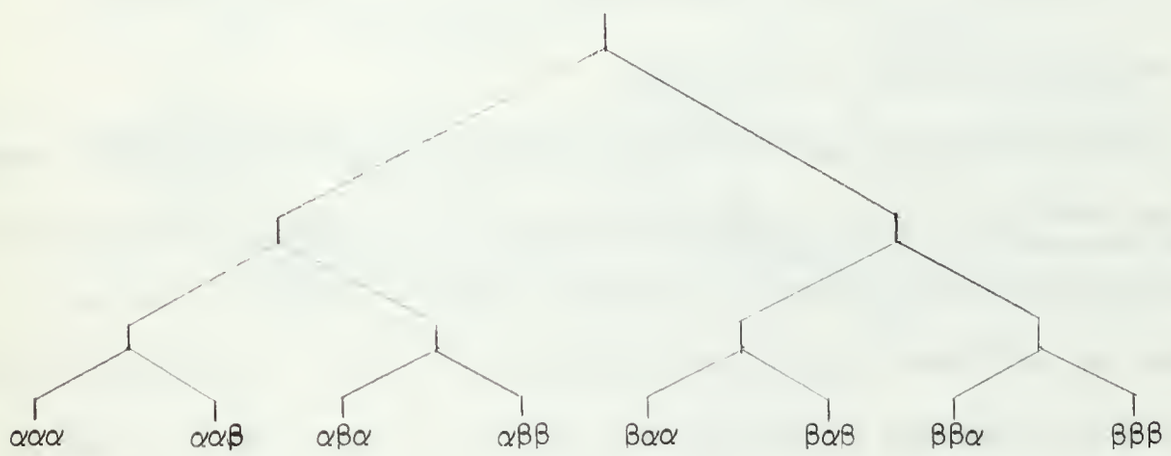

Various rotational frequencies were fed into the above mentioned computer program, and the computed spectra compared with the experimental spectra. It was possible to obtain the frequency of rotation as a function of temperature from this method, and an Arrhenius plot enables the determination of the $\Delta H^{\neq}$ and $\Delta S^{\neq}$ for internal rotation of the methyl group. The results are:

$$\Delta H^{\neq} = 3.0 \pm 0.3 \text{ kcal/mole}$$

$$\Delta S^{\neq} = 6.0 \pm 0.3 \text{ cal/mole deg}$$

The predicted and experimental spectra for a constant magnetic field orientation and varying temperature are shown in Fig. 11A. The dotted line spectra are the calculated spectra. Figure 11B is the Arrhenius plot.

C. LOW TEMPERATURE OBSERVATION

Spectra taken for single crystals of strontium acetate hemihydrate irradiated and observed at liquid nitrogen temperature without warmup show a multiline pattern, as can be seen in Fig. 12, which does not show up again after the crystal has been warmed to -100° C and then re-cooled to -160° C. The orientation of the magnetic field is $\phi = 45^{\circ}$, $\theta = 70^{\circ}$.

D. MOLECULAR ORBITAL CALCULATIONS

Molecular orbital calculations for CH_3CO_2, CH_3CO, and CH_3CHO^- based on the CNDO approximation were made [27,28]. For CH_3CO_2, the calculation predicts the unpaired spin density to be localized in the two oxygen $2p_z$ orbitals, with 0.499 spin density in each. For CH_3CO, the calculation predicts an average spin density on the methyl carbons of 0.01916 which, when multiplied by 500 gauss which is the hydrogen atom coupling constant, yields a 9.6 gauss coupling constant. The spin densities are, for the carboxyl carbon, 0.57; on the oxygen, 0.32 and on the methyl carbon, 0.09. The calculation for CH_3CHO reveals that the average spin density on the methyl hydrogens is 0.014076 which gives a coupling constant of 23.4 gauss. The spin density on the oxygen is 0.35 and on the carboxyl carbon, 0.47. The isotropic coupling constant calculated from McConnell's relation [1] for the inequivalent hydrogen is 10.7 gauss.

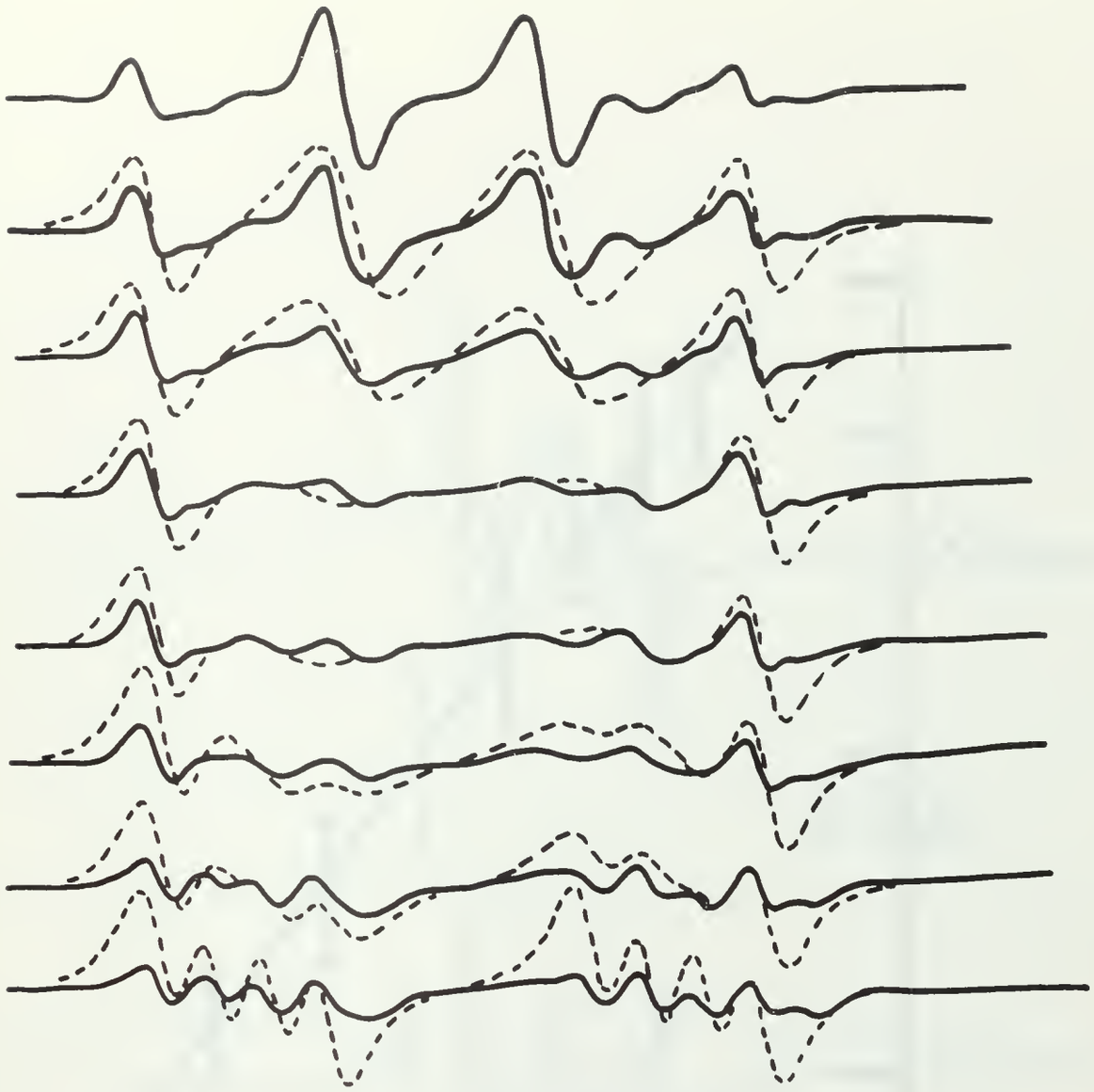

FIGURE IIA

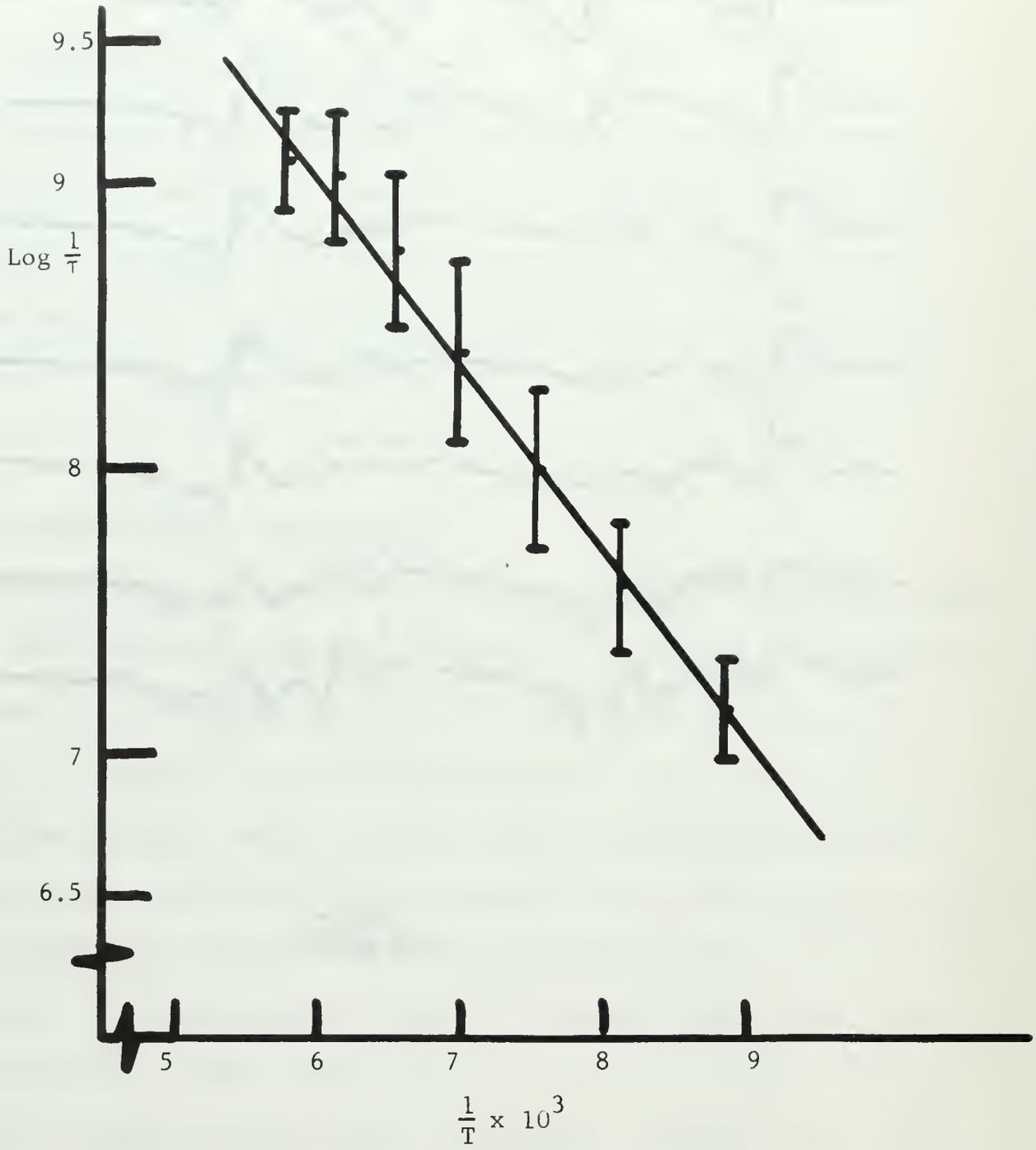

FIGURE 11 B. Arrhenius Plot for determing activation Energy for rotating methyl group in -100° C species.

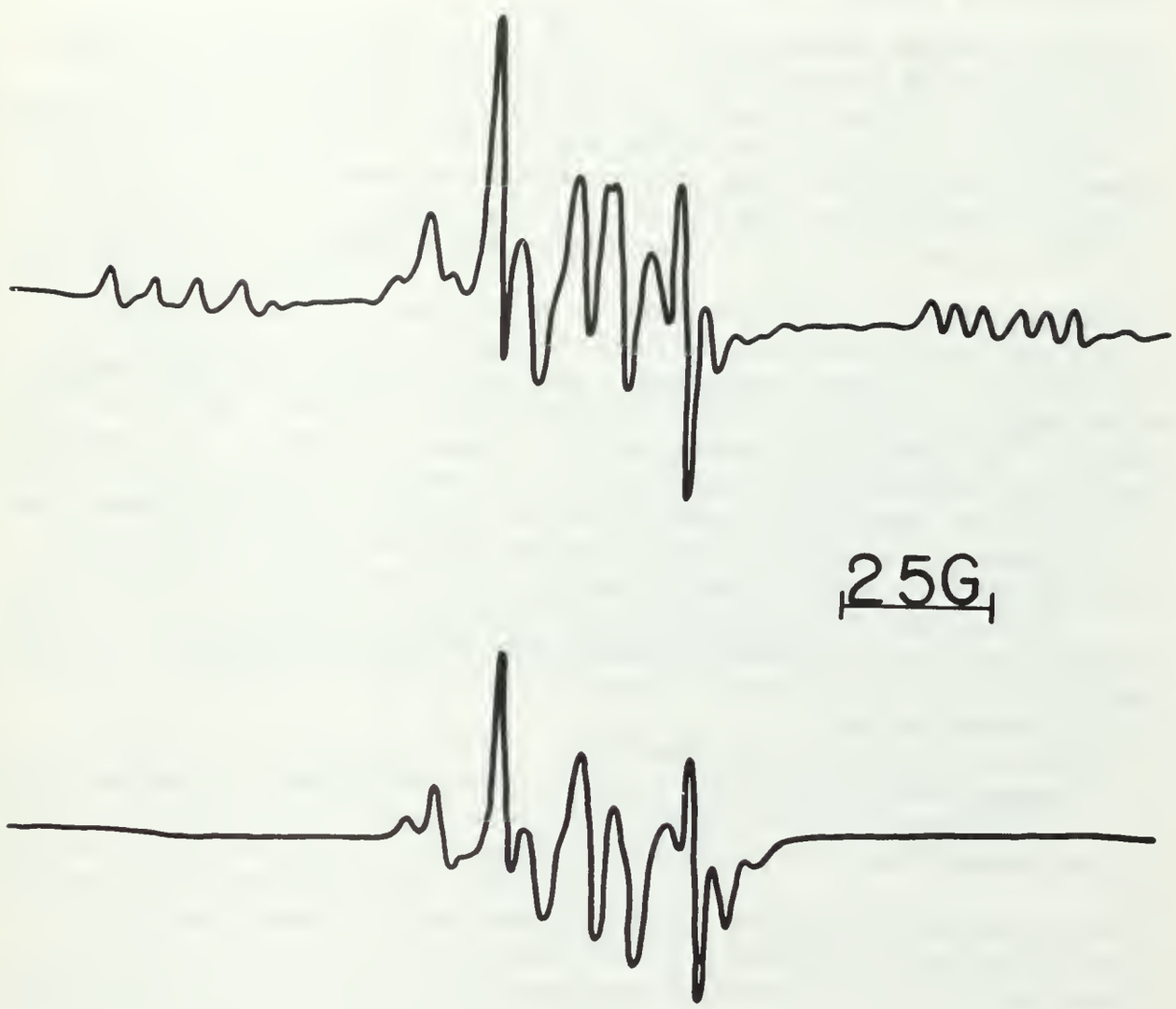

FIGURE 12

E. SUMMARY AND CONCLUSIONS

Radiation damage of strontium acetate hemihydrate single crystals initiates a multistep solid state free radical chemical reaction. At liquid nitrogen temperature to -100° C, a radical of the form CH_3 - X with a^{CH_3} = 9.2 gauss and a pattern of eight equally intense, equally spaced lines exists. The lines exhibit exchange effects to become at -100° C a four line 1:3:3:1 pattern. The exchange is attributed to a rotating methyl group with barrier to internal rotation equal to 3.0 kcal/mole. At room temperature, the species is of the form CH_3CH-X with a^{CH_3} = about 25.2 gauss and a^{H} = about 20. gauss. The spectrum of the room temperature species is two 1:3:3:1 patterns offset from one another because of splitting by a hydrogen atom. In addition, a broad line species exists at room temperature which may be a triplet or a strontium ion.

Comparison of the above results with the molecular orbital calculations shows that the methyl group coupling constant of 9.6 gauss calculated for CH_3CO compares favorably with the 9.2 gauss methyl group coupling constant determined experimentally for the low temperature species. CH_3CO would also be expected to give the same spectrum as the low temperature species. The calculated methyl group coupling constant of 23.4 gauss for CH_3CHO compares favorably with the approximate 25.2 gauss coupling constant for the room temperature species. CH_3CHO would give the pattern described for the room temperature species. CH_3CO_2 is ruled out as a possibility because of its spin density distribution on the two oxygens. Confirmation of the identity of the species in the crystal might be made by irradiating a single crystal of $Sr(CH_3{}^{13}CO_2)_2 \cdot \frac{1}{2}H_2O$ and subsequently examining the ESR spectrum.

APPENDIX A

A MATHEMATICAL MODEL FOR THE MOTIONAL AND EXCHANGE NARROWING OF SPECTRAL LINES

The temperature dependent behavior of the spectra of free radicals with a rotating methyl or $-CH_2$ group may be predicted by a computer program based on a mathematical model developed by Anderson [11] and modified by Sack [12].

The phenomenon of narrowing of magnetic resonance line breadths takes two forms; motional narrowing and exchange narrowing. The mechanism is in principle the same in both motional and exchange narrowing.

The model herein developed assumes that the precessing moments give rise to a radiated electromagnetic wave which is undergoing frequency modulation, because the magnetic interactions act to change the frequency of the precession. The frequency modulation is changing in a random way in time due to the effect of the non-magnetic motions on the magnetic interactions.

It can be shown in general that the spectrum of the radiation from any quantum-mechanical system is given by

(1) $I(\omega) = \text{Trace} \left| \int_{-\infty}^{\infty} \mu(t) e^{-i\omega t} dt \right|^2$ where $\mu(t)$ is the radiating dipole moment matrix in the equation:

(2) $i\hbar \frac{d\mu}{dt} = H\mu - \mu H$ where H is the Hamiltonian.

In any problem involving the type of narrowing dealt with here the Hamiltonian may be split up into three parts:

$$H = H_o + H_p + H_m$$

These three parts are the unperturbed Hamiltonian, the perturbing Hamiltonian--generally just the dipolar interactions between the moments-which does not commute with H_o and thus can change the frequencies radiated by the system over some known range, and the motional Hamiltonian whose characteristic is that it commutes with both H_o and μ, and thus can have no direct effect upon the radiation emitted or absorbed by the system, but does not commute with H_p and thus, by the relation

$$i\hbar \dot{H}_p = [H,H_p] = [H_o,H_p] + [H_m,H_p] \tag{3}$$

brackets denote the commutator can cause a time dependence of H_p. It is this time dependence which narrows out the line broadening which H_p otherwise would cause.

The random frequency modulation picture of the narrowing process can be derived from the following physical assumptions:

(a) equation (1)

(b) equation (3)

(c) $H_m \mu - \mu H_m = 0$

(d) $H_m H_o - H_o H_m = 0$

(e) and, in addition, the assumption that H_p is small enough that it has not important matrix elements connecting different states $E_i^{(0)}$ and $E_j^{(0)}$ of the unperturbed energy H_o.

In any real substance, assumption (e) will not be rigorously true, but may be looked upon as an approximation which, if carefully handled, leads to good quantitative results. Under the above assumptions, the spectral intensity (1) will be computed. Consider one spectral line so that only the element of $\mu(t)$ which connects two unperturbed levels of H_o E_i and E_j need be considered. Then

(4) $$I(\omega)_{i\to j} = \left|\int_{-\infty}^{\infty} \mu_{ij}(t) e^{-i\omega t} dt\right|^2$$

Since that part of the time dependence of $\mu_{ij}(t)$ due to the unperturbed Hamiltonian is known, the following transformation may be performed:

$$\mu_{ij} = \mu'_{ij}(t)\ \exp(i\omega_{ij}^{(0)} t)$$

where

$$\hbar\omega_{ij}^{(0)} = E_i - E_j$$

Now

$$i\hbar \frac{d\mu'}{dt} = [H_m + H_p, \mu] = H_p\mu' - \mu' H_p$$

because of assumption (a) and the fact that the transformation has removed the terms of the time equation (2) for μ which depend on H_o. By use of assumption (e), $\mu'_{ij}(t)$ may be calculated as follows:

$$i\hbar\dot{\mu}'_{ij} = [H_p\mu' - \mu' H_p]_{ij}$$

$$= (H_p)_{ii}\mu'_{ij} - \mu'_{ij}\ (H_p)_{jj}$$

$$\mu'_{ij} = -\, i\Delta\omega_{ij}(t)\mu'_{ij}(t)$$

where

$$\Delta\omega_{ij}(t) = \frac{H_p(t)_{ii} - H_p(t)_{jj}}{\hbar}$$

Then

$$\mu'_{ij}(t) = \mu_{ij}^{(0)}\ \exp(-i\int_o^t \Delta\omega_{ij}(t')dt')$$

This is inserted into the intensity formula (4) which gives, for the lineshape

(5) $$I_{ij}(\omega) \sim \left|\int_{-\infty}^{\infty} \exp(-i(\omega - \omega_{ij}^{(0)})t - i\int_o^t \Delta\omega_{ij}(t')dt')\right|^2$$

$\Delta\omega_{ij}(t)$ is a random function of time; its value at any time depends on the values of the diagonal elements of H_p at that time, and these will change in a random way at a rate controlled by the motional Hamiltonian, as is seen from the time equation (3) (there is no time dependence due to H_o because these are diagonal elements):

$$i\hbar\dot{H}_p = [H_m, H_p]$$

The reason for assuming randomness is that in the important cases the effect of H_p back on H_m can be neglected, so that the motions embodied in H_m appear to the magnetic quantities to be uncorrelated. Equation (5) and the idea of $\Delta\omega_{ij}(t)$ as a random function of time are the basic ideas of the random frequency modulation model of narrowing phenomena. The term $\Delta\omega_{ij}(t)$ is simply a construct, a single function which is meant to embody all of the broadening effects, diagonal as well as off diagonal. In order to find the line shipe, the assumption is made that $\Delta\omega_{ij}(t)$ can be treated as a Markoffian random function.

Equation (5) may be simplified in the following way: Redefine ω as $\omega = \omega - \omega_{ij}^{(0)}$, making ω the frequency deviation from the line center. Introduce the phase deviation $\eta(t)$, which is the integral of the frequency deviation:

$$\eta(t) = \int_0^t \Delta\omega_{ij}(t')dt'$$

Then (5) becomes

$$I(\omega) = \left|\int_{-\infty}^{\infty} e^{-(\omega t - \eta(t))}dt\right|^2$$

Because of convenience, the correlation function form of the Fourier integral will be used. It can be shown that

$$I(\omega) = \int_{-\infty}^{\infty} e^{i\omega\tau} d\tau \int_{-\infty}^{\infty} e^{-i(\eta(t'+\tau) - \eta(t'))} dt'$$

or,

$$(6) \qquad I(\omega) = \int_{-\infty}^{\infty} e^{i\omega\tau} \varphi(\tau) d\tau$$

$\varphi(\tau)$ is called the correlation (or autocorrelation) function and can be written as

$$(7) \qquad \varphi(\tau) = \langle e^{i(\eta(t+\tau)-\eta(t)} \rangle \quad \text{ave. over } t$$

$$= \langle \exp(i \int_{t}^{t+\tau} \Delta\omega_{ij}(t')dt') \rangle \text{ ave over } t$$

This represents the averaged "memory" of the function μ'_{ij} at the time $t + \tau$ for what its state was at a time τ earlier. The problem is to find $\varphi(\tau)$ under the assumption that $\Delta\omega_{ij}(t)$ is Markoffian.

A Markoffian function is a function for which the probability of a given value f_2 at the time t, if the value was f_1 at $t - \Delta t$, is independent of the value of the function at any earlier time than $t - \Delta t$. Thus the probability depends only on the value of the function at the earlier time and not on its past history. The notation used is

$$\text{Probability} = W(f_1 | f_2, \Delta t)$$

If the function is not to vary in a senselessly rapid fashion it is known that W must be proportional to Δt for small Δt unless $f_1 = f_2$. Therefore, W may be written as

$$(8) \qquad W(f_1 | f_2, \Delta t) = \delta(f_1, f_2) + \pi(f_1, f_2) \Delta t$$

where π is the probability per unit time of a transition from f_1 to f_2.

To solve the stated problem, a matrix method of solution is used in which the probabilities $W(f_1, f_2)$ are considered as two dimensional matrices connecting the sets of indices f_1 to f_2. The assumption is made that $\Delta\omega$ has a discrete set of values.

The average in (7) may be written in another way. The interval τ is divided into n equally spaced steps, such that $\frac{\tau}{n}$ is very small compared with the rate of change of $\Delta\omega$. Then

$$(9) \qquad \exp\left[i\sum_{m=1}^{n} \frac{\tau}{n}\,\Delta\omega\left(t + m\frac{\tau}{n}\right)\right] = \exp\left[i\int_{t}^{t+\tau} \Delta\omega(t')\,dt'\right]$$

The probability that $\Delta\omega$ takes on a certain set of values at the various instants in (9) is

$$(10) \qquad W_1(\Delta\omega_1)\, W(\Delta\omega_1 | \Delta\omega_2, \tfrac{\tau}{n}) \times W(\Delta\omega_2 | \Delta\omega_3, \tfrac{\tau}{n}) \times \cdots \times W(\Delta\omega_{n-1} | \Delta\omega_n, \tfrac{\tau}{n})$$

$\varphi(\tau)$ may be found by summing the product of (9) and (10) over all the possible combinations of $\Delta\omega$'s since these are respectively the value and the probability of a given averagand

$$\varphi(\tau) = \sum_{\Delta\omega_1}\sum_{\Delta\omega_2}\sum_{\Delta\omega_3} \cdots \left(\exp\left(i\,\frac{\tau}{n}\sum_{m=1}^{n}\Delta\omega_m\right)\right) \times W_1(\Delta\omega_1) \prod_{m=2}^{n} W(\Delta\omega_{m-1} | \Delta\omega_m, \tfrac{\tau}{n})$$

(11)

$$= \sum_{\Delta\omega_1}\sum_{\Delta\omega_2} \cdots \sum \prod_{m=1}^{n-1} \left(\exp\left(i\frac{\tau}{n}\,\Delta\omega_m\right) \times W(\Delta\omega_m | \Delta\omega_{m+1}, \tfrac{\tau}{n})\right) \exp\left(i\Delta\omega_{nn}\frac{\tau}{n}\right)$$

The central product has the form of a matrix product. It will have this form exactly if the diagonal matrix $\underline{\underline{\Delta\omega}}$ is defined as follows:

$$\underline{\underline{\Delta\omega}}_{ij} = \delta(\Delta\omega_i, \Delta\omega_j) \times \Delta\omega_i$$

The probability matrix is

$$\underline{\underline{W}}\left(\tfrac{\tau}{n}\right)_{ij} = W(\Delta\omega_i | \Delta\omega_j, \tfrac{\tau}{n})$$

$\underline{W}_1(\Delta\omega)$ is a row vector in $\Delta\omega$ space, and $\underline{1}$ $(\Delta\omega)$, the vector all of whose components are unity is a column vector.

Expanding $\exp(i\Delta\omega_n \frac{\tau}{n})$ and neglecting $\Delta\omega_n \frac{\tau}{n}$ with respect to unity, (11) is written as a matrix product multiplied on left and right by row and column vectors respectively:

$$(12) \qquad \varphi(\tau) = \underline{W_1} \cdot (\exp(i \frac{\tau}{n} \underline{\underline{\Delta\omega}}) \underline{\underline{W}}(\frac{\tau}{n}))^{n-1} \cdot \underline{1}$$

Since $\frac{\tau}{n} \Delta\omega$ can be made as small as is necessary, it is permissible to let

$$\exp(i \frac{\tau}{n} \Delta\omega) = \underline{\underline{1}} + i \frac{\tau}{n} \underline{\underline{\Delta\omega}}$$

while from (7) the matrix $\underline{\underline{W}}$ is rewritten in terms of matrix $\underline{\underline{\pi}}$

$$\underline{\underline{W}}(\frac{\tau}{n}) = \underline{\underline{1}} + \underline{\underline{\pi}} \frac{\tau}{n}$$

This gives for (12)

$$(\exp(i \frac{\tau}{n} \Delta\omega) \, W(\frac{\tau}{n}))^{n-1} = (1 + \frac{\tau}{n} (i\underline{\underline{\Delta\omega}} + \underline{\underline{\pi}}))^{n-1}$$

which if n goes to infinity is

$$\exp(\tau(i \underline{\underline{\Delta\omega}} + \underline{\underline{\pi}}))$$

so that (11) becomes

$$\varphi(\tau) = \underline{W_1} \cdot \exp(\tau(i\underline{\underline{\Delta\omega}} + \underline{\underline{\pi}})) \cdot \underline{1}$$

or

$$\varphi(\tau) = \sum_{i,j} \underline{W_i}(\Delta\omega_i) \left\{\exp(\tau(i\underline{\underline{\Delta\omega}} + \underline{\underline{\pi}})\right\} \Delta\omega_i \Delta\omega_j$$

$$(13) \qquad = \underline{W} \exp[\tau(i\underline{\underline{\Omega}} + \underline{\underline{\pi}})] \cdot \underline{1}$$

where the n components of the vector $\underline{W}$ are proportional to the

occupation probabilities of the sites in equilibrium, $\underline{1}$ is a vector with all components equal to unity, $\underline{\underline{\Omega}}$ is a diagonal matrix with elements ω_j and $\underline{\underline{\pi}}$ is a matrix with elements

$$\pi_{jk} = p_{jk} \qquad j \neq k \qquad p = \text{probability}$$

$$\pi_{jj} = -\sum_k p_{jk}$$

For $\varphi(\tau)$ given in (13), equation (6) may be integrated as follows:

$$\int_o^\tau \exp(-i\omega\tau)\varphi(\tau)d\tau =$$

$$\underline{W} \cdot \left[\exp\left\{\tau(\underline{\underline{\pi}} + i\underline{\underline{\Omega}} - i\omega\underline{\underline{E}}_n)\right\}\right]_o^T (\underline{\underline{\pi}} + i\underline{\underline{\Omega}} - i\omega\underline{\underline{E}}_n)^{-1} \cdot \underline{1}$$

where E_n is the unit matrix of order n. For $T\to\infty$ the integral converges only if the real parts of all the eigenvalues of $i\underline{\underline{\Omega}} + \underline{\underline{\pi}}$ are non-positive. From physical arguments it is clear that the integral must converge, so that

$$(14) \qquad I(\omega) \sim 2 \text{ Real } \underline{W} \cdot (i\omega\underline{\underline{E}}_n - i\underline{\underline{\Omega}} - \pi)^{-1} \cdot \underline{1}$$

The calculation as to how the shape of a composite spectral line depends on the transition probabilities between the sites is thus reduced to the inversion of a matrix with complex elements. A computer program to perform the calculation in (14) has been written and begins on the next page.

```
C     THIS PROGRAM CALCULATES THE INTENSITY DISTRIBUTION OF A
C          COMPOSITE SPECTRAL LINE WITH EXCHANGE NARROWING.
C          REFERENCES FOR THE THEORY ARE
C
C          J PHYS SOC JAPAN,9,888
C          MOLECULAR PHYSICS,1,163
C
C
C     WRITTEN BY ROBERT G. GISCH   APRIL  1969
C
C     1ST CARD  SET 1 FOR ESR    2 FOR NMR/NO. OF PLOTS PER
C          GRAPH/NO. OF GRAPHS/NO. OF POINTS TO BE PLOTTED/
C          WIDTH OF FREQUENCY SCALE IN INCHES/DIMENSION OF
C          MATRIX/NO. OF NONZERO OFFDIAGONAL ELEMENTS ABOVE
C          DIAGONAL/LINE WIDTH IN INCHES(THE RECIPROCAL OF
C          T2)/THE HEIGHT,IN INCHES,OF THE HIGHEST ABSORPTION
C          PEAK      I1,I2,I2,I3,3I2,2F10.5
C
C     2ND CARD   VECTOR OF INTENSITIES    6F10.5
C
C     3RD CARD   DIAGONAL MATRIX OF FREQUENCIES OF RESONANCE
C          LINES.  MATRIX ELEMENT AND POSITION OF LINE IN
C          INCHES     6(2I1,F10.5)
C
C     4TH CARD   THE TRANSITION PROBABILITIES TRANSFORMED TO
C          THE INCHES SCALE AS IS THE OTHER DATA.  THE FIRST
C          VALUE OF THE TRANSITION PROBABILITY FED IN WILL
C          DETERMINE THE HEIGHTS OF THE ABSORPTION PEAKS FOR
C          THE REST OF THE PLOTS   6F10.5
C
C     5TH CARD   NONZERO MATRIX ELEMENTS ABOVE DIAGONAL
C          7CI1
C
C     6TH CARD   LABELS FOR EACH PLOT   15 LABELS ON EACH
C          CARD     15A4
C
C     7TH CARD   ADDITIONAL INFORMATION.  TYPE IN AS MANY
C          CARDS AS THERE ARE GRAPHS    6A8
C
C
      IMPLICIT COMPLEX*16(U,O,V,X)
      IMPLICIT REAL*8(A-H,O,P,R-T,W,Y-Z)
      REAL*4 XREQ,XINTEN,YINTEN
      REAL LBL/4H     /
      REAL*8 ITL(12)/'BOX 24, TOLLES
     1                                                  '/
      DIMENSION X(20,20),OMEGA(20,20),UOMEGA(20,20),
     1PROB(20,20),UPROB(20,20),UU(20,20),U(20,20),
     1FREQ(1000),W(20),UW(20),UFREQ(1000),VELEM(20),
     1ZINTEN(1000),HINTEN(1000),IAR(50),RPROB(50),
     1XREQ(1000),XINTEN(1000),YINTEN(1000)
C
C     SET MATRICES TO ZERO
C
      DO 9 I=1,20
      DO 9 J=1,20
      OMEGA(I,J)=0.0
      PROB(I,J)=0.0
      UOMEGA(I,J)=(0.0,0.0)
      UPROB(I,J)=(0.0,0.0)
      U(I,J)=(0.0,0.0)
    9 UU(I,J)=(0.0,0.0)
      EP=1.0E-30
C
C     START TO READ IN DATA
C
      READ 100,KKL,LLL,NNN,NUMPTS,IHIGH,N,MMM,CONST,SCALE
      READ 110,(W(I),I=1,N)
      FREQ(1)=0.0
```

```
      NM1=NUMPTS-1
      AHIGH=IHIGH
      ANMPTS=NUMPTS
      ZINC=(AHIGH/ANMPTS)
      DO 1 I=1,NM1
    1 FREQ(I+1)=FREQ(I)+ZINC
      READ 2,((I,J,OMEGA(I,J)),J=1,N)
      LLNN=LLL*NNN
      READ 110,((BPROB(I)),I=1,LLNN)
      DO 125 I=1,LLNN
  125 BPROB(I)=BPROB(I)/6.283186
      MM=2*MNM
      READ 105,((IAR(I)),I=1,MM)
      REAL*8 TITLE(100,12)
      REAL*8 BLANK(12) /'
     1                                                          '/
      READ LABEL (100)
      READ 120,(LABEL(I),I=1,LLNN)
      DO 300 I=1,NNN
  300 READ 121,(TITLE(I,J),J=7,12)
C
C     END READ IN DATA.  START CALCULATIONS
C
      DO 1001 JT=1,NNN
      DO 1001 II=1,LLL
C
C     SET UP PROBABILITY MATRIX
C
      DO 55 I=1,MM,2
      I1=I+1
      IA=IAR(I)
      IB=IAR(I1)
   55 PROB(IA,IB)=-BPROB((JT-1)*LLL+II)
      DO 58 I=1,N
      DO 58 J=1,N
   58 PROB(J,I)=PROB(I,J)
      DO 22 I=1,N
   22 PROB(I,I)=0.0
      DO 56 I=1,N
      Z=0.0
      DO 57 J=1,N
   57 Z=Z+PROB(I,J)
   56 PROB(I,I)=-Z+CONST/6.283185
C
C     SET UP DIAGONAL TRANSITION FREQUENCY MATRIX AND
C     COMBINE SEPARATE MATRICES TO RESULTANT MATRIX
C
      DO 40 I=1,N
      DO 40 J=1,N
      UOMEGA(I,J)=OMEGA(I,J)
      UOMEGA(I,J)=UOMEGA(I,J)*(0.0,-1.0)
      UPROB(I,J)=PROB(I,J)
      UPROB(I,J)=UPROB(I,J)*(-1.0,0.0)
   40 UU(I,J)=UOMEGA(I,J)+UPROB(I,J)
C
C     DO LOOP WHICH CALCULATES INTENSITIES
C
      DO 1000 M=1,NUMPTS
      DO 11 I=1,N
      DO 11 J=1,N
   11 U(I,J)=UU(I,J)
      UFREQ(M)=FREQ(M)
      UFREQ(M)=UFREQ(M)*(0.0,1.0)
C
C     FREQUENCY ELEMENT ADDED TO IMAGINARY PART OF DIAGONAL
C          ELEMENTS
C
      DO 2 I=1,N
    2 U(I,I)=U(I,I)+UFREQ(M)
C
C     MATRIX INVERSION
C
```

```
      CALL GAUSS4(N,EP,U,X,KER)
C
C     VECTOR OF INTENSITIES*INVERTED MATRIX
C
      DO 6 J=1,N
      Q=(0.0,0.0)
      DO 5 K=1,N
      UW(K)=W(K)
      VMULT=UW(K)*X(K,J)
    5 Q=Q+VMULT
    6 VELEM(J)=Q
C
C     RESULT*UNIT VECTOR
C
      Q=(0.0,0.0)
      DO 7 I=1,N
    7 Q=Q+VELEM(I)
C
C     TAKES REAL PART OF THIS RESULT
C
      S=Q
C
C     INTENSITY IS TWICE THE REAL PART OF THIS RESULT
C
 1000 ZINTEN(M)=2.*S
C
C     END CALCULATIONS.  START COMPUTING GRAPHS
C
      IF(KKL.EQ.1) GO TO 450
C
C     NMR SECTION
C
      DO 550 I=1,M
      XREQ(I)=FREQ(I)
  550 XINTEN(I)=ZINTEN(I)
      IF(JI.GT.1) GO TO 998
      IF(IJ.GT.1) GO TO 998
      TOP=0.0
      DO 444 I=1,NUMPTS
      IF(TOP.GT.XINTEN(I)) GO TO 444
      TOP=XINTEN(I)
  444 CONTINUE
  998 DO 454 I=1,NUMPTS
  454 XINTEN(I)=XINTEN(I)*SCALE/TOP
      IF(IJ.EQ.1)GO TO 765
      DO 766 I=7,12
  766 ITL(I)=BLANK(I)
      GO TO 767
  765 DO 768 I=7,12
  768 ITL(I)=ITITLE(JI,I)
  767 CONTINUE
      LBL=LABEL((JI-1)*LLL+IJ)
      IF(LLL.EQ.1) GO TO 204
      IF(IJ.EQ.1) GO TO 201
      IF(IJ.EQ.LLL) GO TO 202
      CALL DRAW(NUMPTS,XINTEN,XREQ,2,0,LBL,ITL,1.0,1.0,0,0,
     12,2,9,IHIGH,0,LAST)
      GO TO 1001
  201 CALL DRAW(NUMPTS,XINTEN,XREQ,1,0,LBL,ITL,1.0,1.0,0,0,
     12,2,9,IHIGH,0,LAST)
      GO TO 1001
  204 CALL DRAW(NUMPTS,XINTEN,XREQ,0,0,LBL,ITL,1.0,1.0,0,0,
     12,2,9,IHIGH,0,LAST)
      GO TO 1001
  202 CALL DRAW(NUMPTS,XINTEN,XREQ,3,0,LBL,ITL,1.0,1.0,0,0,
     12,2,9,IHIGH,0,LAST)
      GO TO 1001
C
C     ESR SECTION
C
  450 DO 805 I=1,NM1
C
```

```
C    CALCULATES NUMERICAL DERIVATIVE
C
  805 HINTEN(I)=(ZINTEN(I+1)-ZINTEN(I))/ZINC
      DO 551 I=1,M
      XREQ(I)=FREQ(I)
  551 YINTEN(I)=HINTEN(I)
      IF(JI.GT.1) GO TO 999
      IF(IJ.GT.1) GO TO 999
      TOP=0.0
      DO 445 I=1,NM1
      IF(TOP.GT.ABS(YINTEN(I))) GO TO 445
      TOP=ABS(YINTEN(I))
  445 CONTINUE
  999 DO 455 I=1,NM1
  455 YINTEN(I)=YINTEN(I)*SCALE/(TOP*2.)+4.5
      IF(IJ.EQ.1)GO TO 865
      DO 866 I=7,12
  866 ITL(I)=BLANK(I)
      GO TO 867
  865 DO 868 I=7,12
  868 ITL(I)=ITITLE(JI,I)
  867 CONTINUE
      LBL=LABEL((JI-1)*LLL+IJ)
      IF(LLL.EQ.1) GO TO 304
      IF(IJ.EQ.1) GO TO 301
      IF(IJ.EQ.LLL) GO TO 302
      CALL DRAW(NM1,YINTEN,XREQ,2,0,LBL,ITL,1.0,1.0,0,0,2,2,
     1 19,IHIGH,0,LAST)
      GO TO 1001
  301 CALL DRAW(NM1,YINTEN,XREQ,1,0,LBL,ITL,1.0,1.0,0,0,2,2,
     1 19,IHIGH,0,LAST)
      GO TO 1001
  304 CALL DRAW(NM1,YINTEN,XREQ,0,0,LBL,ITL,1.0,1.0,0,0,2,2,
     1 19,IHIGH,0,LAST)
      GO TO 1001
  302 CALL DRAW(NM1,YINTEN,XREQ,3,0,LBL,ITL,1.0,1.0,0,0,2,2,
     1 19,IHIGH,0,LAST)
 1001 CONTINUE
  100 FORMAT(I1,I2,I2,I3,3I2,2F10.5)
  102 FORMAT(6(2I1,F10.5))
  105 FORMAT(70(I1))
  110 FORMAT(6F10.5)
  120 FORMAT(15A4)
  121 FORMAT(6A8)
      STOP
      END


      SUBROUTINE   GAUSS4(N,EP,A,X,KER)
      IMPLICIT COMPLEX*16 (A-D,F-H,O-Y)
      DIMENSION A(20,20),X(20,20)
      DO 1 I=1,N
      DO 1 J=1,N
    1 X(I,J)=(0.0,0.0)
      DO 2 K=1,N
    2 X(K,K)=(1.0,0.0)
   10 DO 34 L=1,N
      KP=0
      Z=0.0
      DO 12 K=L,N
      IF(Z-CDABS(A(K,L)))11,12,12
   11 Z=CDABS(A(K,L))
      KP=K
   12 CONTINUE
      IF(L-KP)13,20,20
   13 DO 14 J=L,N
      S=A(L,J)
      A(L,J)=A(KP,J)
   14 A(KP,J)=S
      DO 15 J=1,N
      S=X(L,J)
      X(L,J)=X(KP,J)
```

```
   15 X(KP,J)=S
   20 IF(CDABS(A(L,L))-EP)50,50,30
   30 IF(L-N)31,34,34
   31 LP1=L+1
      DO 36 K=LP1,N
      IF(CDABS(A(K,L)))32,36,32
   32 RATIO=A(K,L)/A(L,L)
      DO 33 J=LP1,N
   33 A(K,J)=A(K,J)-RATIO*A(L,J)
      DO 35 J=1,N
   35 X(K,J)=X(K,J)-RATIO*X(L,J)
   36 CONTINUE
   34 CONTINUE
   40 DO 43 I=1,N
      II=N+1-I
      DO 43 J=1,N
      S=(0.0,0.0)
      IF(II-N)41,43,43
   41 IIP1=II+1
      DO 42 K=IIP1,N
   42 S=S+A(II,K)*X(K,J)
   43 X(II,J)=(X(II,J)-S)/A(II,II)
      KEP=1
      RETURN
   50 KEP=2
      RETURN
      END
```

BIBLIOGRAPHY

1. Carrington, A., and McLachlan, A. D., Introduction to Magnetic Resonance, Harper and Row, Inc., (1967).

2. McGarvey, B. R., Transition Metal Chemistry, v. 3, p. 90, Marcel Dekker, Inc., (1966).

3. Lounsbury, J. B., J. Chem. Phys., 67, 721 (1966).

4. Jarvis, J. A. J., Acata Cryst., 15, 964 (1962).

5. Jonassen, H. B., Schmitt, D., and Henry, R. A., Copper (II) and Copper (I) Halide Complexes with 1- and 2-Substituted Tetrazoles, unpublished.

6. Garber, L. L., and Brubaker, C. H., J. Am. Chem. Soc., 90, 309 (1968).

7. Brubaker, C. H., J. Am. Chem. Soc., 82, 82 (1960).

8. Bowers, D. M., and Popov, A. I., Inorg. Chem., 7, 1594 (1968).

9. Kuska, H. A., D'Itri, F. M., and Popov, A. I., Inorg. Chem., 5, 1272 (1966).

10. Morton, J. R., Chem. Rev., 64, 453 (1964).

11. Anderson, P. W., J. Phys. Soc. Japan, 9, 316 (1954).

12. Sack, R. A., Mol Phys., 1, 163 (1958).

13. Rogers, M. T., and Kispert, L. D., J. Chem. Phys., 46, 221 (1967).

14. Heller, C., J. Chem. Phys., 36, 175 (1962).

15. Tamura, N., Collins, M. A., and Whiffen, D. H., Trans. Farad. Soc., 62, 2434 (1966).

16. Morton, J. R., J. Chem. Phys., 41, 2956 (1964).

17. Box, H. C., and Freund, H. G., J. Chem. Phys., 44, 2345 (1966).

18. Miyagawa, I., and Gordy, W., J. Chem. Phys., 32, 255 (1960).

19. Horsfield, A., Morton, J. R., and Whiffen, D. H., Mol. Phys., 4, 425 (1961).

20. Horsfield, A., Morton, J. R., and Whiffen, D. H., Mol. Phys., 5, 115 (1962).

21. Miyagawa, I., and Itoh, K., J. Chem. Phys., 36, 2157 (1962).

22. Sinclair, J. W., and Hanna, M. W., J. Phys. Chem., 71, 84 (1967).

23. Sinclair, J. R., and Hanna, M. W., J. Chem. Phys., 50, 2125 (1969).

24. Wells, J. W., and Box, H. C., J. Chem. Phys., 48, 2542 (1968).

25. Tolles, W. M., Crawford, L. P., and Valenti, J. L., J. Chem. Phys., 49, 4745 (1968).

26. Tolles, W., A Computer Program for Calculation of the Hyperfine Coupling Constants and Direction of Symmetry Axis for a Trapped Radical, unpublished.

27. Pople, J. S., and Segal, G. A., J. Chem. Phys., 43, 5136 (1965).

28. Tolles, W., A Computer Program for Molecular Orbital Calculations Using the CNDO Approximation, unpublished.

INITIAL DISTRIBUTION LIST

		No. Copies
1.	Defense Documentation Center Cameron Station Alexandria, Virginia 22314	20
2.	Library, Code 0212 Naval Postgraduate School Monterey, California 93940	2
3.	Commander, Naval Ordnance Systems Command Headquarters, Department of Navy Washington, D. C. 20360	2
4.	Professor William M. Tolles, Code 5417 Department of Material Science & Chemistry Naval Postgraduate School Monterey, California 93940	3
5.	LTJG Robert G. Gisch Department of the Navy Naval Ship Systems Command (Code 08) Washington, D. C. 20360	2
6.	Department of Material Science & Chemistry Naval Postgraduate School Monterey, California 93940	2
7.	LT Leslie P. Crawford USS Springfield (CLG-7) FPO New York, New York 09501	1

DOCUMENT CONTROL DATA - R & D

(Security classification of title, body of abstract and indexing annotation must be entered when the overall report is classified)

1. ORIGINATING ACTIVITY *(Corporate author)*
Naval Postgraduate School
Monterey, California 93940

2a. REPORT SECURITY CLASSIFICATION
Unclassified

2b. GROUP

3. REPORT TITLE
Electron Paramagnetic Responance Study of Copper Halide Tetrazole Complexes and the Free Radicals in Irradiated Strontium Acetate Hemihydrate

4. DESCRIPTIVE NOTES *(Type of report and, inclusive dates)*
Master's Thesis; June 1969

5. AUTHOR(S) *(First name, middle initial, last name)*
Robert G. Gisch

6. REPORT DATE	7a. TOTAL NO. OF PAGES	7b. NO. OF REFS
June 1969	97	28

8a. CONTRACT OR GRANT NO.

b. PROJECT NO.

c.

d.

9a. ORIGINATOR'S REPORT NUMBER(S)

9b. OTHER REPORT NO(S) *(Any other numbers that may be assigned this report)*

10. DISTRIBUTION STATEMENT

This document has been approved for public release and sale; its distribution is unlimited.

Distribution of this document is unlimited

11. SUPPLEMENTARY NOTES

12. SPONSORING MILITARY ACTIVITY
Naval Postgraduate School
Monterey, California 93940

13. ABSTRACT
An EPR study of copper halide tetrazole complexes and x-irradiated strontium acetate hemihydrate has been made. The powder spectra of some of the tetrazole complexes exhibited temperature dependent narrowing and broadening. The one-electron population of the copper d orbital involved in bonding to 2-methyl-5-amino tetrazole has been found to be 0.56 and 0.47, respectively for the chloride and bromide complexes. The g values for these two complexes are consistent with the proposed planar polymeric structure for 2-substituted tetrazole-copper complexes. The species present in single crystals of strontium acetate hemihydrate irradiated and observed at liquid nitrogen temperature to -100° C has a spectrum of four lines of 1:3:3:1 intensity ratio and a^{CH_3}= 11.0 gauss. Temperature dependent exchange behavior of the spectrum for this species is observed and attributed to a rotating methyl group which was found to have $\Delta H^{\neq}$ = 3.0 ± 0.3 kcal/mole and $\Delta S^{\neq}$ = 6.0 ± 0.3 cal/mole deg. for internal rotation. The species present at room temperature has an eight line spectrum consisting of two 1:3:3:1 intensity ratio patterns with a^{CH_3} = 25.2 and a^{H} = 21.3 gauss. Molecular orbital calculations using the CNDO approximation were performed and possible fragments responsible for these spectra are suggested.

14 KEY WORDS	LINK A		LINK B		LINK C	
	ROLE	WT	ROLE	WT	ROLE	WT
Strontium Acetate Hemihydrate						
Electron Paramagnetic Resonance						
Tetrazoles						
Copper Halide						
Radiation Damage						